

Photometric Search for variable stars in the field of two Northern open clusters, DOLIDGE 14 and NGC 1960

Gireesh C. Joshi (✉ gchandra.2012@rediffmail.com)

Research Article

Keywords: Astronomical reduction , NGC 1960, DOLIDGE 14, stellar Variability

Posted Date: September 13th, 2022

DOI: <https://doi.org/10.21203/rs.3.rs-1895965/v1>

License: © ⓘ This work is licensed under a Creative Commons Attribution 4.0 International License.

[Read Full License](#)

Photometric Search for variable stars in the field of two Northern open clusters, DOLIDZE 14 and NGC 1960

Gireesh C. Joshi¹

Email:- gchandra.2012@rediffmail.com

Abstract In the present paper, the CCD time series observations of cluster NGC 1960 and DOLIDZE 14 are performed to search the short periodic variable stars within them. Absolute photometry via secondary standardization transformation has been used to construct the light curves for the detection of pulsation in stars. A comprehensive study of membership of variable stars is discussed along with their classification. A total of 18 and 4 short periodic variables found in the field of NGC 1960 and DOLIDZE 14 respectively. The period and classification of 18 discovered short periodic type variable stars of NGC 1960 are discussed, which consist of one EB, one Planet transit, one $\gamma - Dor$, two $\delta Scuti - \gamma - Dor$, two LADS, two irregular, two rotational, three RRC and four Ellipsoidal type variable stars. In the case of DOLIDZE 14, four discovered variables consist of one miscellaneous, one rotational, two *binary* type variable stars. A comparative analysis of each short periodic variable star has been represented with a set of two comparison stars of similar brightness. In the case of NGC 1960, the 12 selected comparison stars have variation in brightness such that they can be classified as long periodic variable stars. A total of 4 stars are found to be standard stars. The variation in brightness of other twenty comparison stars is non-pulsating with irregular pattern. Very low amplitude pulsations of stars is instrumental errors in nature and seems to be a factor of misleading classification of variable stars. In the case of DOLIDZE 14, variation of brightness in light curves of comparison stars of each variable star is a result of errors during transformation of magnitudes. Membership analysis of variable stars are performed by using their distance, kinematic probability and location in $(U - B)$ vs $(B - V)$ TCD.

Keywords Astronomical reduction – NGC 1960, DOLIDZE 14, stellar Variability

1 Introduction

An open cluster (OCL) is loosely bounded group of up to a few thousand stars caused by the mutual gravitational attraction of cluster members. Such objects are useful for studying stellar evolution because of the similar age and chemical composition of their members. The member stars of the OCL form from a giant molecular cloud. In this connection, a young OCL may be found within its parental molecular cloud and their mutual interaction mechanism is illuminated a process of creation of HII region [A good example of this region is NGC 2244 (Johnson 1962).]. Such regions are active star formation sites and formed young stars with the highest metallicity. The chemical composition or metallicity are used to know the type of stellar population and stars, having high metallicity, belong to Population I (abbreviated as Pop I). As a result, OCLs are host the stars of Pop I. Analysis of observations of the Kepler data-set confirms that the larger, potential gas giants planets are only concentrated around stars of Pop I (Buchhave et al. 2012), whereas smaller planets are found around of stars of all stellar populations. Such planets are traced through the transit method, based on observing the short (≈ 10 hours) periodic ($P = \approx$ months to years) dips in stellar light curves caused by a planet passing in front of the star's disk (Carpano et al. 2003). Thus, fluctuation of stellar light curves becomes an important tool to search exo-planets, however fluctuations of stellar brightness also occur due to other ongoing physical phenomena within their interior and surrounding.

The brightness fluctuations are found for some stars among members of stellar population and such stars

Gireesh C. Joshi

¹Department of Physics, Government Degree College, Kanvaghati (Kotdwar), Pauri-246149

are known to be variable stars. The stellar variability may be arise either due to intrinsic properties (pulsations, eruptions, stellar swelling and shrinking) or extrinsic reasons (eclipsed by stellar rotation by another star or planet etc.). Extrinsic reasons of stellar variability are stellar eclipsing in the binary and triplet stellar systems, properties of interstellar medium, planet transition and accretion process of surrounding matter of stars. Other hand, the change of intrinsic properties of variables are driven by the plasma transportation on the stellar surface, nucleus stellar activities in their interior parts, effect of tidal force on stellar environment due to nearby stars, their masses and ages. As a result, the variable stars are natural targets of study for any civilization due to their correlation between period and total light output, which allowed them to become the first rung in the astronomical distance ladder (Hippke et al. 2015). In this connection, Cepheids of pulsating variables are important indicators of cosmic benchmarks for scaling galactic and extra-galactic distance (Majaess et al. 2009; Freedman & Madore 2010) due to a strong direct relationship between a Cepheid variable's luminosity and pulsation period (Soszynski et al. 2008). Pulsating variables are most important objects due to the periodic expansion and contraction of the surface layers of the stars to maintain its equilibrium. Their census including pulsators and binaries, can provide important clues to stellar evolution and the host star clusters (Luo et al. 2012). The several classes of pulsating variables are largely found at instability strip region of the Hertzsprung-Russell (HR) diagram. Since, pulsating variables has an associated instability strip (Dupret et al. 2004) above the MS, therefore, an OCL provides an opportunity to estimate the properties of its stellar variables through its own characteristic parameters.

Since the detection and magnitude estimation of the most fainter stars are primary affected by their nearby brighter stars, the knowledge of flux contamination of the stars in the science frame of any cluster is absolutely necessary to investigate the nature of instrumental pseudo-variability. In this connection, we need a cluster region fulfilled by brighter stars and NGC 1960 is found a potential candidate for such study. Other hand, deep time-series photometry is further bound by exposure time to investigate the variable stars within enhanced fainter stars field of any cluster. For this purpose, DOLIDZE 14 is found a potential candidate.

In this background, we are carried out analysis of the time series observations of NGC 1960 and DOLIDZE 14 to search the variable stars within them. The previous parametric studies of both clusters are given in the Section 2. The observational details of these clusters are given in the Section 3. The methodology of

data reduction is discussed in the Section 4. The identification procedure of variable stars of DOLIDZE 14 and NGC 1960 is given in the Section 5. The Fast-Fourier analysis of variables discuss in Section 6. The mean-proper motions and kinematic membership probabilities for both clusters are described in Section 7. A comparative study of variable stars with parameters of both clusters is discussed in Section 8. A detail description of identified stars of cluster DOLIDZE 14 and NGC 1960 is given in Sections 9 and 10. Results, discussion and Conclusion are described in Sections 11 & 12.

2 Previous studies and antecedents of stellar variability

2.1 NGC 1960

This cluster is situated in the Constellation Auriga and has been studied in the past by many authors. The Center coordinates (α , δ) for this cluster is estimated to be ($05^h : 36^m : 20.8^s$, $+ 34^\circ : 08' : 31''$) and ($05^h : 36^m : 20.2^s$, $+ 34^\circ : 08' : 06''$) by Sharma et al. (2006) and Cantat & Anders (2020), respectively. The photoelectric and photographic study of this cluster was done by Johnson & Morgan (1953) and Barkhatatova et al. (1985), respectively. The proper motion study of this cluster was carried out by Meurers (1958), Chian & Zhu (1966) Sanner et al. (2000) and Joshi et al. (2020) [JO20 now onward]. The photometric study of this cluster has been performed by Sanner et al. (2000), Nilakshi et al. (2002) and Sharma et al. (2006). Its angular size is computed to be 16 arcmin and 10.3 arcmin by Joshi & Tyagi (2015a) and Cantat & Anders (2020), respectively. Kharchenko et al. (2004) and Conrad et al. (2017) reported the radial velocity as -1.2 km/s and -1.18 km/s, respectively. The log-age of this cluster is reported by Kharchenko et al. (2004), Joshi & Tyagi (2015a) and JO20 as 7.62 (yr), 7.35 (yr) and 7.44 (yr), respectively. The near-IR photometric study of NGC 1960 was carried out by Hasan et al. (2005). Sharma et al. (2008) studied the mass function and effect of photometric binaries in the region of cluster NGC 1960. Using Lithium depletion boundary technique, Jeffries et al. (2013) determined the age of this cluster.

A complete *UBVRIJHKW₁W₂* photometric catalogue has been represented by Joshi & Tyagi (2015a) by complying the PPMXL catalogue with the obtained *UBVRI* standard photometric magnitude of gathered data on date of 30 Nov, 2010 and same data set was further analyzed by JO20 for their absolute/standard

photometric analysis. By utilizing catalogues of various data-sets, a comprehensive photometric analysis of this cluster along with the long-term variability is represented by them. A total of 76 variable stars of NGC 1960 has been identified by JO20, and their analysis confirmed 72 periodic variables among them, 59 are short period ($P < 1 d$). They used absolute photometry for detection of variable stars, in which instrumental errors are surely added due to magnitude translation. In the case of this cluster, flux of detected nearby fainter stars of brighter stars will be contaminated during its deep CCD photometric observations. Such circumstances surely lead an over-estimation in the detection of short periodic variable stars.

In the view of above antecedents, author is motivated to perform time series observations of this cluster with low exposure times of 05, 06 and 10 seconds .

2.2 DOLIDZE 14

In the database of WEBDA, the center coordinates, $(\alpha, \delta)_{J2000}$, of DOLIDZE 14 is $(04^h : 06^m : 36.0^s, + 27^\circ : 26' : 00.0'')$ as per work of Alter et al. (1970). ? has been studied nature of stellar enhancement around the celestial coordinates, $(04^h : 06^m : 36.0^s, + 27^\circ : 26' : 00.0'')$ $_{J2000}$ and they depicted results as per infrared photometric analysis of stars within DOLIDZE 14. This cluster have stellar enhancement in the B-band of USNB1.0, whereas it does not show any stellar enhancement in the infra-red bands (Joshi & Tyagi 2015b). In this connection, they have been estimated the values of $(\alpha, \delta)_{J2000}$ and (μ_x, μ_y) as $(04^h : 06^m : 26.7^s, + 27^\circ : 22' : 26.7'')$ and $(-0.15 \pm 0.34 \text{ mas/yr}, - 7.79 \pm 0.41 \text{ mas/yr})$, respectively. ? are estimated the values of radius, reddening and distance as $9.6 \pm 0.2 \text{ arcmin}$, $0.32 \pm 0.02 \text{ mag}$ and $1.67 \pm 0.14 \text{ kpc}$ respectively. It is a suitable field for analysis of deep CCD-photometric observations due to have a system of fainter stars and it is also non-standardized in optical photometry.

For the name of cluster DOLIDZE 14, Dias et al. (2014) gave the values of center coordinates $(\alpha, \delta)_{J2000}$, and proper motions (μ_x, μ_y) as $(04^h : 06^m : 43.0^s, + 27^\circ : 32' : 34.0'')$ and $(1.71 \text{ mas/yr}, -0.88 \text{ mas/yr})$ respectively. This given center of cluster is separated by 08 arcmin with respect to that of Alter et al. (1970) and this cluster is denoted by $C 0403 + 273$ in the database of SIMBAD. As a result, author concludes that cluster DOLIDZE 14 $[(04^h : 06^m : 26.7^s, + 27^\circ : 22' : 26.7'')_{J2000}]$ and cluster $C 0403 + 273 [(04^h : 06^m : 43.0^s, + 27^\circ : 32' : 34.0'')_{J2000}]$ are historically distinct regions and may have cluster properties.

The nature of absolute photometry for time series observation for any cluster may be understood with

respect to secondary standard stars within it and its comparative analysis can be represented using a non-standardized system of stars. As per above antecedents of DOLIDZE 14 $[(04^h : 06^m : 26.7^s, + 27^\circ : 22' : 26.7'')_{J2000}]$, it is potential system of stars for such comparative analysis.

3 Data Collection and Extraction

To detect the short periodic pulsation of stars of target cluster, we need time series observation of the whole night as per availability of target in the telescopic field of view. The time series observations of studied clusters, DOLIDZE 14 and NGC 1960, are carried out by utilizing observational facilities of 1.04-m Sampurnanad telescope of ARIES, Manora Peak, Nainital. The CCD camera of 1.04-m Sampurnanad telescope of ARIES covers $15 \times 15 \text{ arcmin}^2$ field of view of the target objects. Since, the size of both clusters is more than the telescopic field of view, therefore, we have performed an analysis of the time series observations of the core regions of both clusters. In this connection, the bias and flat frames are also observed for each observational night of studied clusters. The weather conditions (seeing, humidity, wind flow, passing clouds etc.) and declination of target object affect the receiving flux of stars. Thus, the quality of observational data is most important to perform the crucial task of identification of variables. In this connection, the selection procedure of exposure times and observational details of clusters are given as below,

3.1 Characteristics of observational data of NGC 1960

To identify short periodic pulsations of stars within core region of NGC 1960, time series observations are carried

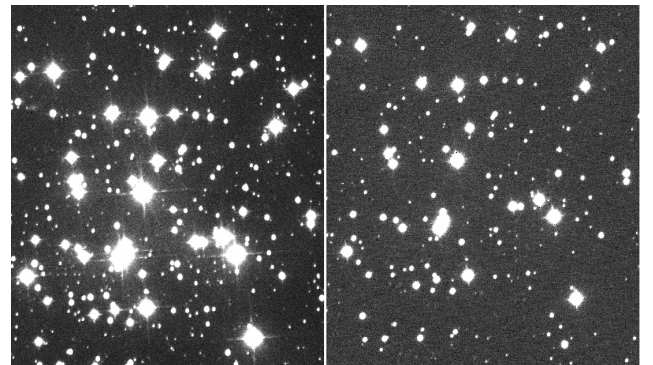


Fig. 1 In the left and right panels of this figure, the science frames of 60 seconds and 10 seconds are shown for core-region of NGC 1960, which are observed on date 24-01-2012 and 11-12-2013 respectively.

Table 1 The observation details of collected data of DOLIDZE 14 and NGC 1960 for searching variable stars within them.

1. DOLIDZE 14					
S.No.	Date	Observation Band (Frames)	Observation Time & Mode	No. of Frames	Exposure Time
1.	13-10-2014	I	3.25 hours, Slow	52	150 Sec.
2. NGC 1960					
S.No.	Date	Observation Band (Frames)	Observation Time & Mode	No. of Frames	Exposure Time
1.	30-11-2010	U	-, Slow	002	300 Sec.
		B		002	300 Sec.
		V		002	200 Sec.
		R		002	200 Sec.
		U		002	060 Sec.
2.	24-01-2012	V	3.5 hours, Slow	070	60 Sec.
3.	11-12-2013	V (150 frames)	5.4 hours, Slow	050	05 Sec.
				050	10 Sec.
				050	20 Sec.
4.	20-12-2013	V (080 frames)	7.6 hours, Slow	040	06 Sec.
				040	60 Sec.
5.	12-01-2015	V (200 frames)	7.2 hours, Slow	100	05 Sec.
				100	20 Sec.
6.	08-02-2015	V (140 frames)	5.6 hours, Slow	140	20 Sec.

out in V-band during 5 observation nights (2012-2015). It contains ten stars of a visual magnitude brighter than 10 (Jeffries et al. 2013), one B-type Variable of 9th magnitude (Delgado et al. 1984), 178 down to magnitude 14 (Sanner et al. 2000) and 38 members have infrared excess (Smith & Jeffries 2012). Thus, our telescopic field of view for NGC 1960 is fulfilled by several brighter stars. We found that these brighter stars almost saturated during an exposure time of 5 seconds. In this regard, the value of exposure time of 5 seconds in V-band becomes too high for saturation counts of the brighter stars of NGC 1960 and leads flux contamination for near by fainter stars of brighter stars in the observed science frames using the facility 1.04-m telescope at ARIES, Nainital. Similarly, an exposure time of 1 second is too low value to collection the stellar information for fainter stars of NGC 1960 below 17 mag in V-band. Environmental influences (seeing, air flow, humidity, passing clouds etc.) and high declination of the target cluster from zenith further reduce the value of stellar magnitude and alter the rate of stellar detection. As a result, different number of faint stars are detected in different science frames of NGC 1960. To overcome the detection problem of faint stars, we performed the deep CCD photometric observation of core region of NGC 1960, with exposure times of 10, 20 and 60 seconds. We need continuous observations of 4-6 hours or more, therefore, the science frames of NGC 1960 have been captured in the alternating order of low (5 or 6 seconds) and high (10 or 20 or 60 seconds) exposure times during the observation session of night. Thus, the exposure time plays a major role to

collect the stellar information. The visual picture of science frames for exposure times of 10 and 60 seconds for NGC 1960 are shown in the right and left panels of Figure 1. In these figures, flux contamination of nearby stars of brighter stars are found more for science frame with exposure times of 60 seconds than that of 10 seconds. The detail of exposure times and brief description of present used data is given in Table 1.

3.2 Characteristics of observational data of DOLIDZE 14

The deep CCD photometric observations are needed for stellar detection in the field of view of DOLIDZE 14 due to its faintness. In this connection, this cluster is observed in I-band on the date 13 Oct, 2014 through 1.04-m Sampurnanand telescope at ARIES, Manora Peak, Nainital. A total of 52 science frames are captured over a period of 3 hours 15 min. It was noted that the positions of the stars slightly shifted during exposure time of 300 seconds. Consequently, the observations of longer exposure times for open cluster has been avoided. A time series observation of this cluster with an exposure time of 150 seconds is done by the author. The visual picture of science frame of DOLIDZE 14 is shown in right panel of Figure 2 and details of its observations is listed in Table 1.

4 Methodology of Data reduction

The raw science frame of target contains the electronic noise, counts of nonuniform pixel sensitivity and cosmic

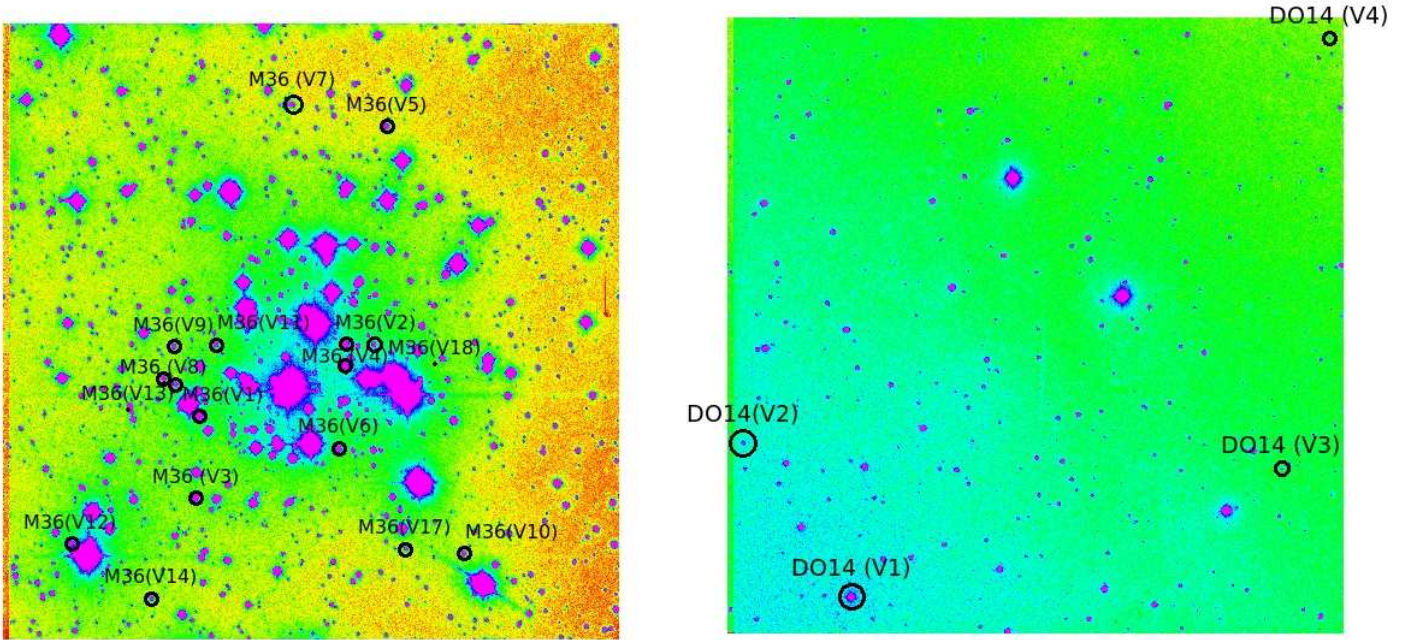


Fig. 2 In the left and right panels, the science frames are shown for core-region of NGC 1960 (M36) and DOLIDZE 14 in V-band and I-band as observed on date 30-11-2010 and 13-10-2014 respectively. The exposure times for them were taken to be 200 seconds and 150 seconds, respectively. The present detected variable stars are depicted by open circle in these Finding charts.

rays. The data reduction procedures (cleaning, standardization) of observed data would required to overcome these defects from science frames of targets to search variable stars within them. The brief detail of data reduction of observed frames of studied cluster is given below,

4.1 Cleaning of raw science frames

The bias-subtraction, flat fielding and cosmic-ray reduction are compulsory steps in the cleaning procedure of raw science frames. In this connection, the bias correction and flat-fielding of observed science frames of NGC 1960 and DOLIDZE 14 have been carried out by using those bias and flat frames, which are observed in the same observational night of object. We are also utilized bias and flat frames of nearby night for the science frames of NGC 1960 due to the lack of these frames in observed data. For this purpose, the ‘ZERO-COMBINE’ and ‘FLAT-COMBINE’ tasks of ‘IRAF’ package are utilized. ‘COSMICRAYS’ task of ‘IRAF’ software are used to remove cosmic rays from the science frames. Such cleaned science frames are used to compute instrumental magnitudes of detected stars in observed field of view of the targets. These instrumental magnitudes of stars may convert into the standard magnitudes by either the transformation coefficients of

the standardization night or solution of linear fitting of secondary standard stars of cluster.

4.2 standardization Details for NGC 1960

In order to perform consistent photometry from night to night on the aligned images (Joshi et al. 2012), we need a master list of stars from science frames of target cluster, which have the best seeing and coverage of the observed core region of both clusters. By using prescribed telescope in Section 3.1, the photometric observations of the open star cluster NGC 1960 were obtained on the night of 30 Nov, 2010. The bias and twilight flat frames were obtained during the observational night for the normalization of the CCD pixels. Two Landolt’s standard fields *SA95* and *PG0231+051* (Landolt 1992) were also observed on the same observational night. A total of ten frames of the cluster with 2 frames each in *U*, *B*, *V*, *R* and *I* filters having exposure times of 300, 300, 200, 200 and 60-sec were obtained in respective passbands. All the observations were taken in 2×2 binning mode for improving the signal-to-noise ratio. The basic steps of image processing such as bias subtraction, flat fielding and cosmic-ray removal were performed through *IRAF*¹. Photometry analysis

¹Image Reduction and Analysis Facilities (IRAF) is distributed by the National Optical Astronomy

was done using *DAOPHOT II* profile fitting software (Stetson 1987). To determine the difference between aperture and profile-fitting magnitudes, the construction of an aperture growth curve was carried out by *DAOGROW* program (Stetson 1992). The instrumental magnitude was translated into standard magnitude using the following transformation equation:

$$m_i = M_i + z_i + c_i \times color + k_i \times X \quad (1)$$

where z_i, c_i, m_i, M_i and k_i are respectively represent the zero-point, colour-coefficient, aperture instrumental magnitude and extinction coefficient for different pass-bands. The $(U-B)$, $(B-V)$, $(V-R)$ and $(R-I)$ colours were used to determine instrumental magnitudes in U , B , V , R and I pass-bands, while X is used for air-mass. The zero-point, colour coefficient and extinction coefficient for $UBVRI$ pass-bands are listed in Table 2.

In Fig. 3(a), we have shown the variation of standard deviations with brightness of stars in different pass-bands. It is clear from this figure that the errors are higher at the fainter end. The calibrated residuals in magnitude (difference between standard and calibrated magnitude) of standard stars in the Landolt's field are shown in Fig. 3(b). The standard deviation of the calibration are respectively estimated as 0.083, 0.071, 0.047, 0.030 and 0.049 mag in U , B , V , R and I filters.

4.3 Astrometry and alignment of frames

The coordinates of detecting stars are found in the term of pixels through $2k \times 2k$ charge couple device (CCD) camera of 1.04-m telescope. Since, the pixel coordinates of identified stars are shifting due to telescopic motion and observed field of view, therefore, 'GEOMAP' and 'GEOTRAN' tasks of IRAF software are utilized to align the all science frames for analysis. In the astrometry, pixel coordinates of detected stars have been transformed into celestial coordinates (α_{2000} , δ_{2000}) by using

Observatories, operated by the Association of Universities for Research in Astronomy Inc., under cooperative agreement with the National Science foundation.

Table 2 The zeropoint, colour-coefficient and extinction-coefficient for different passbands. The colour-coefficients and extinction coefficients listed here.

Filter	zeropoint(z_i)	colour	
		coefficient(c_i)	extinction coefficient(k_i)
U	8.16 ± 0.01	-0.05 ± 0.01	0.55 ± 0.02
B	5.81 ± 0.02	-0.01 ± 0.02	0.29 ± 0.03
V	5.43 ± 0.01	-0.08 ± 0.01	0.15 ± 0.01
R	5.23 ± 0.01	-0.09 ± 0.02	0.09 ± 0.02
I	5.63 ± 0.02	0.01 ± 0.01	0.07 ± 0.02

a linear astrometric solution as derived by matching a set of common stars between present reference catalogue and the 2MASS catalogue with the rms value of about one arcsec in RA and DEC. A total of 29 and 63 common stars are selected in the observed field of DOLIDZE 14 and NGC 1960 respectively. For this purpose, the visualization of images and access to catalogues has been done by 'SKYCAT' tool of ESO². The *CCMAP* and *CCTRAN* tasks of *IRAF* were used for these transformation.

4.4 A complete $UBVRIJHKW_1W_2$ catalogue for NGC 1960

The compilation of $UBVRI$ and IR photometry provide an opportunity to derive basic parameters of an open cluster under study. The IR photometric magnitudes of stars were extracted from the two-micron all sky survey [*2MASS*](Skrutskie et al. 2006) and Wide-field mid-IR Survey Explorer [*WISE*](Wright et al. 2010) surveys within 1 arcsec rms deviation of stellar positions estimated by $UBVRI$ photometry.

Our photometry resulted in a total of 1605 stars within $13' \times 13'$ field of the cluster NGC 1960 in which 447, 1088, 1424, 1583 and 1532 stars were found in U , B , V , R and I bands, respectively. The observed field of NGC 1960 is only central region due to the limited field of view, therefore author combined present photometric data with the Sharma et al. (2006). To make the best use of these two photometries, we choose the magnitudes with minimum errors from both the photometries, in each individual passband. That is done in $UBVR$ bands, however, in I band, we took the magnitudes from Sharma et al. (2006) as our I band images were of poor quality and data shows a linear trend and shift. Combining our catalogue with the 2MASS and WISE data, we prepared a combined catalogue of 18461 stars in $UBVRIJHKW_1W_2$ bands and used for the further analysis. Here, we note that not all the magnitudes are available for all the stars. The entire catalogue is given in Table 3

4.5 Translation of stellar magnitude for DOLIDZE 14

It is noted that OCL, DOLDIZE 14 have not calibrated by any standardized field at yet. In this background, data set of detected stars of its first science frame of our work considered to be its reference catalogue for further analysis of stellar variability within it. Other observed science frames of DOLIDZE 14 are calibrated according to this reference catalogue by using the technique of

²www.eso.org/sci/observing

Table 3 A complete UBVRJHKW₁W₂ catalogue of the stars in the field of the cluster NGC1960. Columns 2 and 3 are RA and DEC of stars, respectively in epoch J(2000). From column 4 to 13, we give photometric magnitudes in UBVRJHKW₁W₂ passbands.

<i>ID</i>	<i>RA</i>	<i>DEC</i>	<i>U</i>	<i>B</i>	<i>V</i>	<i>R</i>	<i>I</i>	<i>J</i>	<i>H</i>	<i>K</i>	<i>W₁</i>	<i>W₂</i>
1	05:34:10.44	34:13:03.4	99.990	9.760	8.120	99.990	-	5.219	4.403	4.200	3.843	3.330
2	05:36:23.05	34:10:33.0	8.276	9.106	8.291	-	-	8.864	8.923	8.942	8.920	8.964
3	05:34:12.63	34:38:00.3	99.990	8.450	8.370	99.990	-	8.151	8.168	8.179	8.083	8.126
4	05:37:50.94	33:58:02.1	7.920	8.460	8.440	99.990	-	8.101	7.942	7.776	7.269	6.974
5	05:38:24.39	34:10:27.0	99.990	8.630	8.470	99.990	-	8.127	8.119	8.108	8.042	8.080
.
.

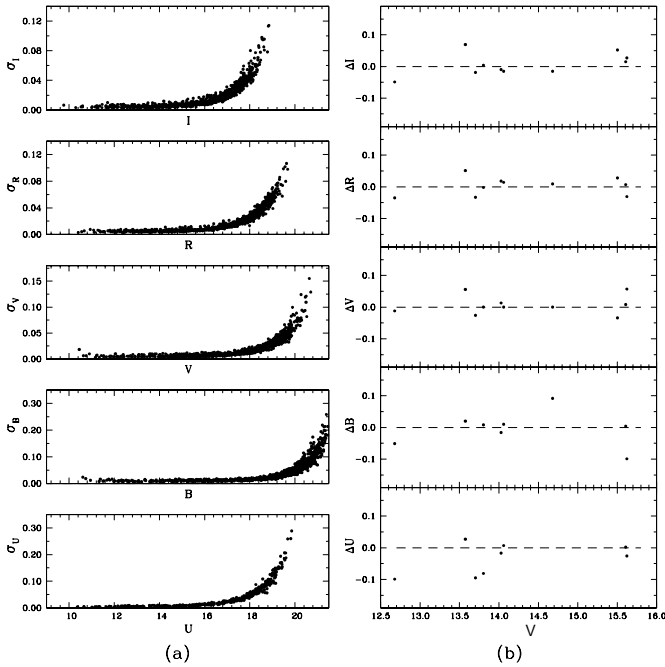


Fig. 3 In left panels, we present standard deviation (errors) of stars as a function of brightness. The right panels show difference between our estimated magnitudes with that of the Landolt’s magnitude for the standard stars in UBVRJ passbands. The black dashed line represents zero shift.

SSM to reduce atmospheric-effect and estimation-errors of stellar magnitudes during the data collection. In this connection, we need a set of common stars, which are available in their reference frame and science frames. These common stars are used to find out a linear fit between the reference magnitudes and instrumental magnitudes of each frames, assuming that most of the stars have stable magnitude. For this purpose, we reject those stars for linear fitting, which deviate more than 3σ limit of deviations of fitting. Resultant linear solution are used to transform instrumental magnitudes of stars of studied clusters into their absolute magnitudes.

4.6 Secondary standardization method for NGC 1960

The secondary standardization method [SSM Joshi et al. (2015)] is effective to estimate the absolute stellar magnitudes of NGC 1960 through the calibrated magnitudes of its stable stars. The magnitudes of variable stars are rapidly varying compare to other stars and identified variable stars were not utilized for such calibration. In this connection, the master list of stable stars of observed core region of NGC 1960 is prepared by using method as discussed for DOLIDZE 14.

5 Identification of variable stars

The collective information of variation of stellar magnitude with time is known to be light curve of target. If, we find the deviation of absolute magnitudes of star more than 3σ limit of mean value of its light curve, then, it will be considered a possible candidate of variable stars. As a result, the possible variable candidates identify by inspecting of their light curves (Sariya et al. 2014). In this connection, the shapes of light curves of a variable star give valuable information for examining the nature of stellar variability and underlying physical processes producing the brightness changes. The light curves of regular variables (such as Cepheids) are repeating with a constant value of time (i.e. its period).

Mira variables have less regular light curves with large amplitudes of several magnitudes, while semi-regular variables are less regular with the smaller amplitudes (Samus et al. 2017). In this connection, amplitudes of light curves of irregular variables does not occur after a fixed time interval and shape of their light curves have found in an uncertain pattern. The amplitude or period of the pulsations can be related to the luminosity of the pulsating stars and shape of their light curves can be an indicator of the pulsation mode (Wood & Sebo 1996). As a result, pulsating variables are distinguished by their periods of pulsation and the shapes of their light curves (Lata et al. 2014). For this purpose, the interesting magnitude ranges of CMD plane of NGC 1960 and DOLIDZE 14 are discussed as follow,

5.1 Need of Transformation of stellar magnitudes during search of variable stars

To be useful, the comparison stars not only must be near the variables and be constant in brightness, but they must also have approximately the same colours and magnitudes. If, the comparison stars have been chosen correctly in the case of isolated stars of field of view of any target object, then the difference between their magnitudes should be approximately constant along the night. It is also noted that effect of contamination depends on exposure times as well as stellar distances from brighter stars. Since, the observed field of NGC 1960 is highly contaminated due to presence of brighter stars at its core region, therefore, magnitude variation for nearby stars of these bright stars is varied as per physical distance and stellar orientation. In addition, Exposure time of its science frames is not constant during observation, which further leads different amount of flux contamination for them. Eventhough, the flux contamination is also changed for same exposure time as per distance of cluster from Zenith. As a result, difference of instrumental magnitudes of nearby similar comparison stars of detected variables is not found approximately constant for NGC 1960. Since, DOLIDZE 14 is observed in I-band only, therefore, the comparison stars of its variable is searched in such a way that their I-magnitudes may closer to corresponding variables. Such detected comparison stars are found physically far away from their variable. As a result, detected comparison stars are not correctly suitable for variables of DOLIDZE 14. The number of detected stars of any science frame also depends on its exposure time. A total of 200 ± 50 stars are detected in each frame for DOLIDZE 14, whereas, 1800-3000 stars are found in the science frames of NGC 1960. The absolute stellar magnitudes is computed for instrumental

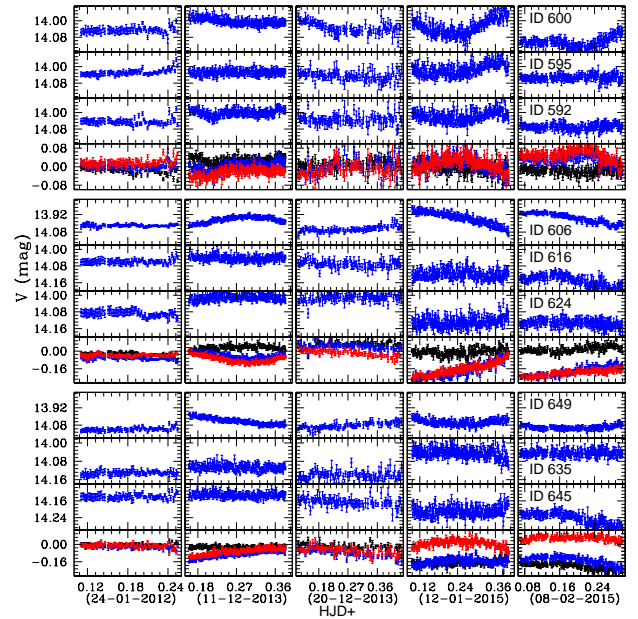


Fig. 4 The panels represent the stellar light curves for star IDs 592, 595, 600, 606, 616, 624, 635, 645 and 649 of cluster NGC 1960. The star IDs 592 and 595 are selected comparison stars for Potential variable (V_1 , Star ID 600). The star IDs 616 and 624 are selected comparison stars for Potential variable (V_2 , Star ID 606). The star IDs 635 and 645 are selected comparison stars for Potential variable (V_3 , Star ID 649).

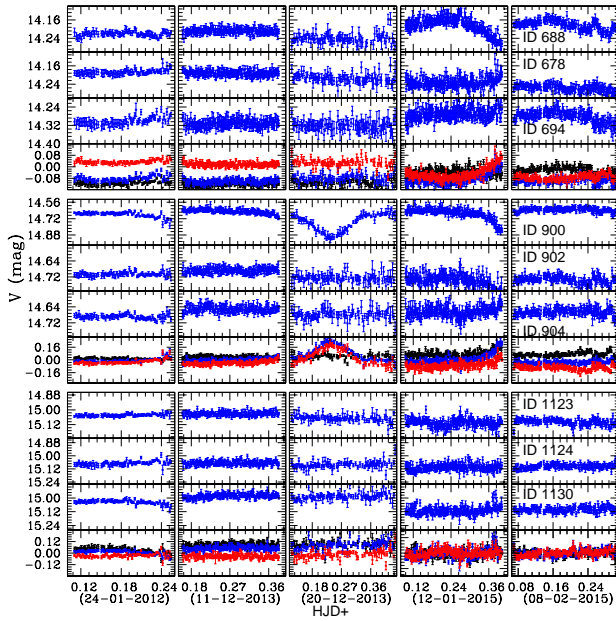


Fig. 5 The panels represent the stellar light curves for star IDs 678, 688, 694, 900, 902, 904, 1123, 1124 and 1130 of cluster NGC 1960. The star IDs 678 and 694 are selected comparison stars for Potential variable (V_4 , Star ID 688). The star IDs 902 and 904 are selected comparison stars for Potential variable (V_5 , Star ID 900). The star IDs 1124 and 1130 are selected comparison stars for Potential variable (V_6 , Star ID 1123).

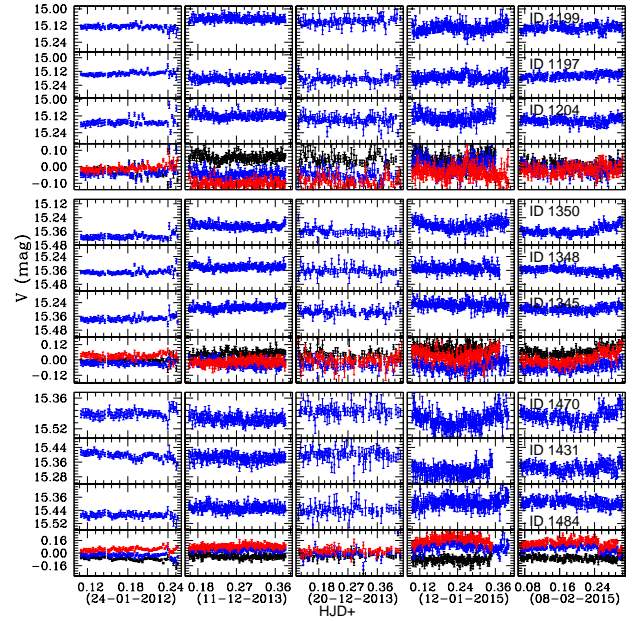


Fig. 6 The panels represent the stellar light curves for star IDs 1197, 1199, 1204, 1345, 1348, 1350, 1431, 1470 and 1484 of cluster NGC 1960. The star IDs 1197 and 1204 are selected comparison stars for Potential variable (V_7 , Star ID 1199). The star IDs 1345 and 1348 are selected comparison stars for Potential variable (V_8 , Star ID 1350). The star IDs 1431 and 1484 are selected comparison stars for Potential variable (V_9 , Star ID 1470).

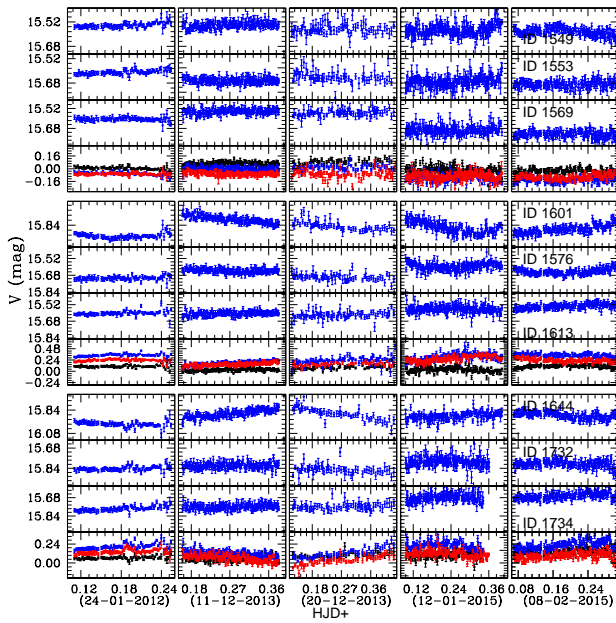


Fig. 7 The panels represent the stellar light curves for star IDs 1549, 1553, 1569, 1576, 1601, 1613, 1644, 1732 and 1734 of cluster NGC 1960. The star IDs 1553 and 1569 are selected comparison stars for Potential variable (V_{10} , Star ID 1549). The star IDs 1576 and 1613 are selected comparison stars for Potential variable (V_{11} , Star ID 1601). The star IDs 1732 and 1734 are selected comparison stars for Potential variable (V_{12} , Star ID 1644).

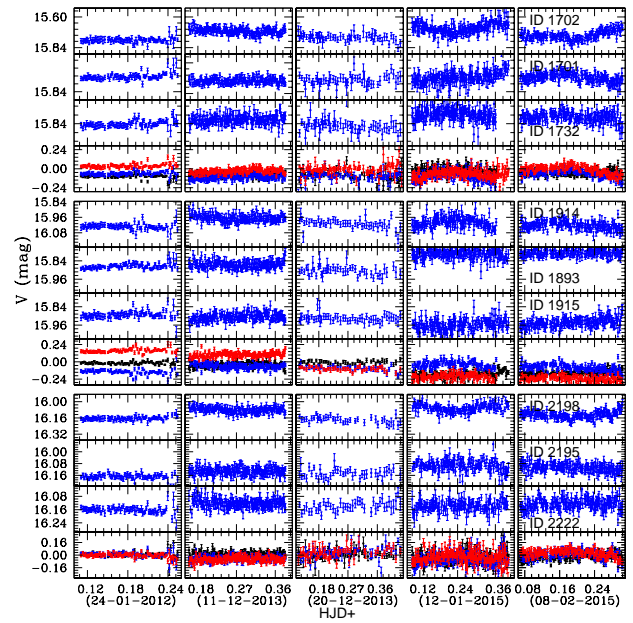


Fig. 8 The panels represent the stellar light curves for star IDs 1701, 1702, 1732, 1893, 1914, 1915, 2195, 2198 and 2222 of cluster NGC 1960. The star IDs 1701 and 1732 are selected comparison stars for Potential variable (V_{13} , Star ID 1702). The star IDs 1893 and 1915 are selected comparison stars for Potential variable (V_{14} , Star ID 1914). The star IDs 2195 and 2222 are selected comparison stars for Potential variable (V_{15} , Star ID 2198).

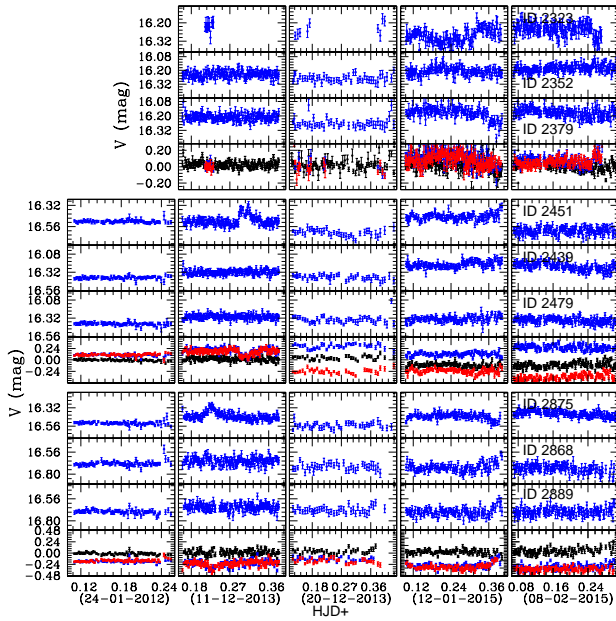


Fig. 9 The panels represent the stellar light curves for star IDs 2323, 2352, 2379, 2439, 2451, 2479, 2868, 2875 and 2889 of cluster NGC 1960. The star IDs 2352 and 2379 are selected comparison stars for Potential variable (V_{16} , Star ID 2323). The star IDs 2439 and 2479 are selected comparison stars for Potential variable (V_{17} , Star ID 2451). The star IDs 2868 and 2889 are selected comparison stars for Potential variable (V_{18} , Star ID 2875).

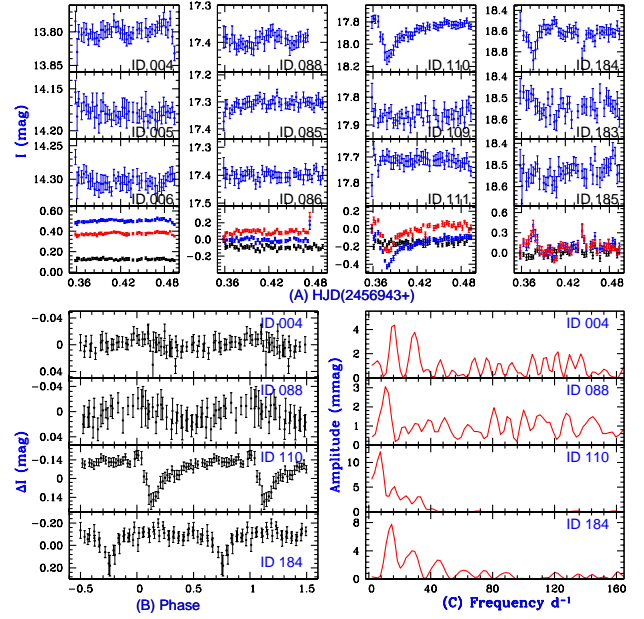


Fig. 10 (A):- We represent the light curves of identified variables (ID 004, ID 088, ID 110, ID 184) and their corresponding comparison stars in the field-view of DOLIDZE 14. The HJD time of observations are shown in x-axis whereas y-axis is shown apparent magnitudes of stars in I -filter. (B):- The panels show light-pholded-curves or phase diagrams of identified variables. The value of phase and amplitude ($mmag$) of stellar variability are shown in the x-axis and y-axis respectively. (C):- The frequency spectrum of identified variables of DOLIDZE 14 are depicted here. The frequency (d^{-1}) and amplitude ($mmag$) of variables are represented in x-axis and y-axis respectively.

magnitudes of each science frame for NGC 1960 by application of SSM. Other hand, the reference frame of DOLIDZE 14 did not standardized with respect to any standard field stars. The stellar magnitudes of detected stars of each science frame of DOLIDZE 14 are translated with respect to its reference frame, therefore, SSM methodology provides the apparent stellar magnitudes for DOLIDZE 14 by considering the uniform variation in stellar magnitudes due to various sky conditions for the entire session of observations.

However, additional errors are surely added to the light curves due to transforming to the standard or reference system. Amount of these additional errors are negligible with compare to effect of contamination on instrumental magnitudes. These transformed stellar magnitudes are used to generate the light curves of stars.

5.2 Limitation of Differential Photometry

The approximate constant environment parameter (seeing, humidity etc.) and dark night is essential conditions for standardization. The varying sky conditions during observations generate noise and instrumental errors, which lead to the scattering of data points in the stellar light curves. The sky conditions change with unexpectedly, the transformation coefficients also vary accordingly during the process of SSM of each science frame. As a result, the irregular variation of stellar magnitudes are still remains, though, these variations are very close to estimated stellar magnitudes with respect to standard and reference catalogue. Such variation can also produce the pseudo stellar variability. Thus, stellar light curves carry the information of stellar variability as well as irregular variations of instrument errors, noise and their aliases. A varied sky condition alters the equal amount of stellar fluxes for all isolated stars as detected in a science frame of target. The different orders of variation is obtained in instrumental magnitudes for stars as per their different amount of fluxes. Such variation may produce different pattern of pseudo-variability in light curves for stars, having different magnitude. Although, same pattern of pseudo-variability is found for nearby isolated stars, having approximate similar in terms of colour and magnitudes. Hence, such irregular variations have the same pattern for similar isolated stars and can be narrowed down through the differential photometry. However, the selection of nearby comparison stars (having magnitude and colour approximately similar to variable star) is a basic requirement in differential photometry. Unfortunately, we are not found such nearby comparison stars for variables of NGC 1960 due to the impact of contamination of brighter stars. In addition, we

are found distinct comparison stars for variable stars of DOLIDZE 14. In differential photometry, the exact confirmation of stellar variability can not possible through the light curve of a star due to absence of its nearby comparison stars. In these circumstances, the variables stars are detected after visual inspection of light curves as per standard magnitudes via absolute photometry. The possible candidacy of variable stars is assigned for stars, having a variation of amplitudes above the 3σ limit of its mean in light curves. After the visual inspection of light curves of detected stars of both clusters, we found a total of 4 and 18 possible variable candidates in the observed field of DOLIDZE 14 and NGC 1960, respectively.

5.3 Validity test approach of SSM via differential photometry

In the present work, we have not found ideal nearby comparison stars for detected variable stars of both clusters and we are not capable to apply differential photometry for such case. Only those stars has been selected as variable stars, which have magnitude variation greater than three times of estimation errors of magnitudes in their light curves as constructed after SSM approach. Since, there are no available information of influence of the pseudo variability in detected variables, therefore, we analyze light curves of stable stars, having same order of magnitudes of variables, for tracing the pattern of pseudo-variability among them. Since, the transformation of instrumental magnitudes leads additional errors, therefore, the scattering is further increased in data points of their light curves. Such transformation makes a weak information of stellar variability. Thus, it may possible that a selected stable comparison star for any variable star have weak information of stellar variability below 3σ limit of its light curves. As a result, we have been avoided the practice of selection of a single stable star for comparing its light curve that of potential variable. For accuracy, we have selected two stable comparison stars for each potentially variable star within their science frames as observed for each cluster. It is kept in the point of view that the magnitude difference of selected comparison stars (possibly stable) and their corresponding variable stars is minimum. The pixel coordinates, differences of stellar magnitudes and colours of identified variables and their comparison stars are listed in the Table 4 and Table 5.

Difference values of pixel coordinated and colours of selected stable stars are conforming their non-usability for study of variable stars via differential photometry. However, comparative analysis of their light curves becomes a tool to understand the nature of instrumental

errors and to trace the impact of pseudo-variability. In this background, the differential photometry has been performed for confirming the nature of variable stars above the 3σ limit of variation of instrumental errors of detected stars within DOLIDZE 14 and NGC 1960.

5.4 Nature of stellar light curves

The light curves of potential variable stars and their corresponding stable stars are depicted in Figure 2 to 8. To distinguish the instrumental variations from stellar light curves, the stellar magnitudes are subtracted from each other and resulting curves are defined as comparative light curves. The light curves for each variable and its selected comparison stars (set of three stars) have shown in the different panels of these figures. In this connection, each set of stars have four panels. Top panel shows the light curve of potential variables and middle panels show the light curves of selected comparison stars. The fourth panel of each set have three lines of blue, red and black colour for representing the comparative light curves. The blue and red lines are shown the field subtracted light curves of variable through comparison stars, whereas black line represents the difference of stellar magnitudes of selected comparison stars. A constant spacing of comparative light curves is obtained for stable comparison stars, while the varied spacing of these curves confirms the signature of stellar variability. Since, obtained information of stellar variability changes rapidly with the sky and weather conditions, therefore, we can not find stellar variability of the order of *mmag* during session of bright moon and observational nights, having fog and high humidity. As a result, we have selected smoother light curve to compute the period of identified variable after the visual inspection of individual light curve of each observational night.

5.5 Comparative Analysis of SSM with essential conditions of Differential Photometry

The major characteristics of comparative light curves of present comparison stars of variable stars of NGC 1960 are obtained as below,

(1)- The shifted and varied magnitude differences are found in comparative light curves of comparison stars of variable stars V_1 , V_2 and V_{12} .

(2)- A constant value of magnitude difference is found in comparative light curves of comparison stars of variable stars V_6 , V_8 and V_{11} during observations of individual night. However, shifting of magnitude difference is altered night to night observations.

(3)- A constant value of magnitude differences is found

in comparative light curves of comparison stars of variable V_3 , V_4 , V_9 , V_{14} and V_{17} during the observations on date 24-01-2012, 11-12-2013 and 20-12-2013. Similarly, a shifted and constant value of magnitude differences is obtained in light curves of these stars during the observations on date 12-01-2015 and 08-02-2015.

(4)- A constant value of magnitude differences is found in comparative light curves of comparison stars of variable V_5 , V_9 , V_{10} , V_{13} , V_{15} , V_{16} and V_{18} during the observations.

Thus, detected variable stars of NGC 1960 are listed in four different groups as per comparative light curves of their comparison stars. After deep investigation of Table 4 and Table 5, we have not found any criteria of geometric distribution of comparison stars and their colour-difference values for separating variable stars of NGC 1960 into these obtained groups. It indicates that there are no need of comparison stars for any variable star after implication of SSM approach. In nutshell, the present SSM approach is seems to be reliable to evaluate the stellar variable nature within studied clusters.

6 Fourier Transform of variables and their Pulsations

The light curves of stars contain aliases frequencies due to the interaction of pulsation of variables and the noise or instrumental errors. Such summation of noise and pulsation signal of variable is removed through the utilization of comparison star during differentiate photometry and becomes an effective method to reduce the uncertainty of detected pulsation signal in the scattered data points of light curves of variables. After confirming the pulsation signal of stars, we need a periodogram to estimate the spectral density of a signal during the pulsation signal processing. Now days, the periodogram are computed from the stellar light curves through the implemented of algorithms such as LombScargle folding (Lomb 1976; Scargle 1982), Box-fitting Least Squares or "BLS" (Kovacs et al. 2002) and Plavchan (Plavchan et al. 2008). Standard and advanced Fourier transform techniques are useful in the analysis of astrophysical time series of very long duration (Ransom et al. 2002) due to their better computing ability. The Lomb-Scargle algorithm is a variation of the Discrete Fourier Transform (DFT), in which a time series is decomposed into a linear combination of sinusoidal functions³. This algorithm has been implemented by us to detect pulsation of variables and constructed the Fourier-Discrete-

³exoplanetarchive.ipac.caltech.edu/docs/pgram

Table 4 Variable IDs for cluster are listed in first column . The pixel coordinates for variable and its two comparison stars are given in second, third and fourth columns. Fifth, sixth and seventh columns indicate the **separation pixel-distances** for potential short periodic variable stars and its comparison stars.

1:- DOLIDZE 14						
Va. ID.	Pixel coordinates for Variable V	Pixel Coordinates for I^{st} com. C1	Pixel coordinates for II^{nd} com. C2	ΔD V & C1	ΔD V & C2	ΔD C1 & C2
V_1	(206.40, 060.40)	(403.50, 867.50)	(372.00, 575.00)	830.818	540.589	294.191
V_2	(026.20, 315.80)	(243.50, 224.50)	(743.50, 688.50)	235.701	808.347	682.126
V_3	(920.80, 274.00)	(586.50, 599.50)	(314.00, 527.50)	466.591	657.623	281.851
V_4	(1001.00, 988.80)	(085.50, 891.50)	(400.00, 247.50)	920.656	954.320	716.691
2:- NGC 1960						
V_1	(326.39, 371.36)	(330.42, 136.68)	(591.11, 108.45)	234.715	373.093	262.214
V_2	(569.17, 491.82)	(443.96, 350.19)	(315.14, 932.95)	189.041	509.045	596.828
V_3	(320.79, 236.69)	(537.44, 628.87)	(447.95, 306.69)	448.043	145.154	334.378
V_4	(569.16, 455.81)	(647.30, 237.98)	(840.54, 176.63)	231.421	389.344	202.745
V_5	(637.19, 853.38)	(573.39, 374.35)	(484.63, 809.77)	483.260	158.671	444.375
V_6	(558.23, 316.76)	(897.74, 312.71)	(450.51, 967.25)	339.534	659.349	792.740
V_7	(481.46, 890.25)	(872.18, 373.21)	(066.07, 073.17)	648.068	916.607	860.138
V_8	(266.90, 435.15)	(225.75, 295.63)	(365.48, 075.02)	145.462	373.379	261.138
V_9	(284.21, 488.30)	(743.37, 037.84)	(558.63, 768.81)	643.228	392.418	753.954
V_{10}	(766.26, 144.03)	(660.10, 216.48)	(330.21, 960.67)	128.526	925.765	814.031
V_{11}	(354.26, 490.63)	(257.50, 399.39)	(767.47, 741.93)	132.993	483.626	614.331
V_{12}	(112.94, 160.52)	(546.62, 058.62)	(857.20, 025.36)	445.491	756.433	312.356
V_{13}	(287.39, 424.57)	(784.75, 180.53)	(546.62, 058.62)	554.006	448.464	267.522
V_{14}	(247.05, 069.18)	(652.48, 558.88)	(943.23, 490.50)	635.751	813.743	298.683
V_{15}	(278.49, 425.25)	(440.69, 644.26)	(641.41, 863.99)	272.533	569.389	297.607
V_{16}	(077.18, 1032.47)	(774.83, 722.69)	(462.34, 572.85)	763.334	599.666	346.557
V_{17}	(669.95, 151.53)	(419.01, 544.23)	(301.97, 842.46)	466.030	782.811	320.374
V_{18}	(617.01, 490.98)	(513.65, 218.19)	(458.72, 856.76)	291.715	398.561	640.928

Table 5 Variable IDs for cluster are listed in first column . V-magnitudes of variable stars of NGC 1960 and I-magnitudes of variable stars of DOLIDZE 14 are given in second column. Values of colour, $(B - V)$, of variable stars of NGC 1960 and colour, $(J - K)$ of variable stars of DOLIDZE 14 are listed in third column. Fourth, fifth and sixth columns indicate the difference of magnitudes for potential variable and its comparison stars. Seventh, eighth and ninth columns represent delta differences of prescribed colour values. In case of NGC 1960, V-magnitudes are standard magnitude as reported by Joshi & Tyagi, 2015.

1:- DOLIDZE 14								
Va. ID.	I-magnitude for Variable V	Colour (J-K) for Variable V	$\Delta_{I_{mag}}$ V & C1	$\Delta_{I_{mag}}$ V & C2	$\Delta_{I_{mag}}$ C1 & C2	$\Delta_{(J-K)}$ V & C1	$\Delta_{(J-K)}$ V & C2	$\Delta_{(J-K)}$ C1 & C2
V ₁	13.784 ± 0.015	0.264 ± 0.038	-0.370	-0.483	-0.113	-0.394	-0.487	-0.093
V ₂	17.385 ± 0.030	0.656 ± 0.072	0.013	0.011	-0.002	-0.206	-0.173	0.033
V ₃	17.804 ± 0.055	0.139 ± 0.183	0.003	-0.006	-0.009	0.074	0.301	0.227
V ₄	18.501 ± 0.086	0.595 ± 0.139	0.032	-0.001	-0.033	0.396	-0.133	-0.529
2:- NGC 1960								
Va. ID.	V-magnitude for Variable V	Colour (B-V) for Variable V	$\Delta_{V_{mag}}$ V & C1	$\Delta_{V_{mag}}$ V & C2	$\Delta_{V_{mag}}$ C1 & C2	$\Delta_{(B-V)}$ V & C1	$\Delta_{(B-V)}$ V & C2	$\Delta_{(B-V)}$ C1 & C2
V ₁	14.007 ± 0.004	0.511 ± 0.005	-0.032	-0.017	-0.015	-0.164	-0.078	0.086
V ₂	14.020 ± 0.004	0.520 ± 0.007	0.029	0.044	-0.015	-0.415	-0.152	0.263
V ₃	14.127 ± 0.005	0.991 ± 0.007	-0.040	-0.011	-0.029	0.418	0.438	0.020
V ₄	14.215 ± 0.008	0.569 ± 0.008	-0.036	0.019	-0.022	-0.055	-0.145	-0.123
V ₅	14.674 ± 0.006	0.674 ± 0.007	0.002	0.005	-0.003	-0.013	0.025	0.038
V ₆	15.060 ± 0.004	0.743 ± 0.006	0.001	0.007	-0.007	-0.088	-0.269	-0.181
V ₇	15.155 ± 0.009	1.522 ± 0.014	-0.001	0.004	-0.005	0.760	0.509	-0.251
V ₈	15.345 ± 0.005	0.766 ± 0.005	-0.013	-0.008	-0.005	-0.920	0.072	0.992
V ₉	15.497 ± 0.004	0.938 ± 0.005	-0.042	0.011	-0.053	-0.164	-1.216	-1.052
V ₁₀	15.592 ± 0.004	0.778 ± 0.005	0.005	0.022	-0.017	-0.064	-0.027	0.037
V ₁₁	15.668 ± 0.005	0.966 ± 0.007	-0.034	0.011	-0.045	0.326	-0.103	-0.429
V ₁₂	15.711 ± 0.007	0.946 ± 0.009	0.089	0.091	0.012	0.135	-0.002	-0.123
V ₁₃	15.769 ± 0.004	0.820 ± 0.006	-0.001	0.031	0.009	-0.364	-0.032	0.373
V ₁₄	15.969 ± 0.004	0.944 ± 0.007	-0.017	0.001	-0.018	-0.669	-0.061	0.608
V ₁₅	16.197 ± 0.005	0.809 ± 0.008	-0.002	0.016	-0.018	-0.387	-0.217	0.170
V ₁₆	16.279 ± 0.006	0.984 ± 0.008	0.022	0.041	-0.019	-0.001	-0.709	-0.708
V ₁₇	16.369 ± 0.007	1.070 ± 0.011	-0.007	0.022	-0.029	0.285	-0.840	-1.125
V ₁₈	16.673 ± 0.007	1.112 ± 0.009	-0.007	0.006	-0.013	0.242	0.224	-0.018

Table 6 The first column shows variable ID of variables within studied clusters. The second and third columns represent *RA* and *DEC* respectively. The values of period of detected variable stars are estimated through the PERIOD04 and PerSea Software as listed in fourth and seventh columns respectively.

1:- DOLIDZE 14						
Variable ID	RA	DEC	Period (days) PERIOD04	Amplitude (mmag)	Power [PERIOD04]	Period (days) PerSea
V_1	4 : 07 : 12.11	27 : 15 : 17.7	0.0599±0.0067	270	04.356	0.0606±0.0068
V_2	4 : 06 : 56.99	27 : 13 : 13.4	0.0939±0.0195	474	03.051	0.0714±0.0074
V_3	4 : 07 : 02.32	27 : 24 : 27.8	0.1349±0.0359?	311	12.169	0.1428±0.0173?
V_4	4 : 06 : 21.87	27 : 26 : 01.5	0.0674±0.0085	327	07.793	0.0714±0.0062
2:- NGC 1960						
Variable ID	RA	DEC	Period (days) PERIOD04	Amplitude (mmag)	Power [PERIOD04]	Period (days) PerSea
V_1	05 : 36 : 25.11	34 : 06 : 10.2	0.3057±0.0815	102	66.948	0.4000±0.1055
V_2	05 : 36 : 17.85	34 : 09 : 14.8	0.2246±0.0599	165	56.576	0.6250±0.0274
V_3	05 : 36 : 33.33	34 : 06 : 05.4	0.3598±0.0001	086	99.261	0.4000±0.2086
V_4	05 : 36 : 20.05	34 : 09 : 14.6	0.3115±0.1168	062	35.608	0.2857±0.0706
V_5	05 : 35 : 55.79	34 : 10 : 07.6	0.3182±0.0848	248	34.752	0.2857±0.0454 (2.4949 : ^{*2})
V_6	05 : 36 : 28.54	34 : 09 : 05.8	0.1528±0.0194	069	24.174	0.1538±0.0369
V_7	05 : 35 : 53.49	34 : 08 : 09.6	0.1747±0.0254	065	23.504	0.1695±0.0154
V_8	05 : 36 : 21.20	34 : 05 : 25.4	0.2864±0.0007	073	65.225	0.2857±0.0947
V_9	05 : 36 : 17.96	34 : 05 : 38.7	0.2667±0.0006	095	48.289	0.4629±0.0399
V_{10}	05 : 36 : 39.17	34 : 11 : 42.8	0.1886±0.0003	074	31.753	0.2404±0.0226
V_{11}	05 : 36 : 17.84	34 : 06 : 31.8	1.1053±0.0007	124	185.267	1.098±0.1033
V_{12}	05 : 36 : 37.89	34 : 03 : 27.5	0.8538±0.0004	084	93.789	0.6667±1.0505
V_{13}	05 : 36 : 21.85	34 : 05 : 40.9	0.3057±0.0815	076	35.455	0.2857±0.0762
V_{14}	05 : 36 : 43.52	34 : 05 : 08.8	0.2665±0.0711	077	13.036	0.2222±0.0775
V_{15}	05 : 36 : 21.81	34 : 05 : 34.1	0.3039±0.0810	072	23.669	0.2041±0.0105
V_{16}	05 : 35 : 44.69	34 : 03 : 03.4	0.3005±0.0801	087	22.739	0.2941±0.0171
V_{17}	05 : 36 : 38.67	34 : 10 : 29.8	-----	-----	-----	-----
V_{18}	05 : 36 : 17.92	34 : 09 : 51.1	-----	-----	-----	-----

Table 7 The detail of amplitude change in identified variables of DOLIDZE 14 and NGC 1960. Amplitude of the stellar Pulsation of variable stars computed through are listed in third column, as computed through the visual inspection of Phase-curve of variables.

1:- DOLIDZE 14					
Variable ID	Normalized Amplitude	Amplitude (mmag) [Phase Curve] [PERIOD04]	Normalized Amplitude	Structural Index [Phase Curve]	Variable Type
V_1	19.588	052	03.772	0.193	<i>miscellaneous</i>
V_2	27.265	082	04.716	0.173	<i>Rotational</i>
V_3	17.468	352	19.771	1.132	Binary?
V_4	17.675	381	20.593	1.165	Contact Binary
2:- NGC 1960					
Variable ID	Normalized Amplitude	Amplitude (mmag) [Phase Curve] [PERIOD04]	Normalized Amplitude	Structural Index [Phase Curve]	Variable Type
V_1	07.282	120	08.567	1.176	$\delta - Scuti - \gamma - Dor$
V_2	11.768	096	06.847	0.581	$\gamma - Dor$
V_3	06.088	089	06.299	1.035	<i>RRC</i>
V_4	04.362	111	07.808	1.790	$\delta - Scuti - \gamma - Dor$
V_5	16.901	254	17.309	1.024	Planet Transit
V_6	04.582	087	05.777	1.261	<i>Ellipsoidal</i>
V_7	04.289	071	04.685	1.092	<i>Ellipsoidal</i>
V_8	04.757	139	09.058	1.904	<i>Rotational</i>
V_9	06.130	123	07.937	1.294	<i>RRC</i>
V_{10}	04.746	099	06.349	1.334	<i>LADS</i>
V_{11}	07.914	204	13.020	1.645	<i>EB</i>
V_{12}	05.347	154	09.802	1.833	<i>Rotational</i>
V_{13}	04.820	118	07.483	1.553	<i>Ellipsoidal</i>
V_{14}	04.822	089	05.573	1.156	<i>Ellipsoidal</i>
V_{15}	04.445	097	05.989	1.347	<i>LADS</i>
V_{16}	05.344	224	13.760	2.574	<i>RRC</i>
V_{17}	----	----	----	----	Irregular
V_{18}	----	----	----	----	Irregular

periodogram (FDP). In this connection, the 'PERIOD04'⁴ and 'PerSea'⁵ software are utilized to estimate the period of new identified variable stars. 'Period04' is dedicated to the statistical analysis of large astronomical time series with gaps and offers tools to extract the individual frequencies from the multi-periodic content. Other hand, 'PerSea' is based on the analysis of variance (ANOVA) algorithm. In the Table 3, we listed the resultant estimated period of variables through the both software. The phase-folded diagrams of detected regular variables are constructed by utilizing the values of pulsation period as per 'Period04'. The phase-folded light curves of variables of DOLIDZE 14 have been depicted in the Figure 8(B), whereas these curves of variables of NGC 1960 are shown in the Figure 9. In these diagrams, the phase values of any variable at time t is defined to the decimal part of $(t - JD)/P$, where JD and P represent the Initial Julian Date and Period of the variables. In this connection, the value of JD is 2455951.11037 and 2456943.35851 for NGC 1960 and DOLIDZE 14 respectively.

6.1 Smoothness of phase diagrams and change in amplitude of pulsation

There is too much of a scattering of data points in the original phase diagrams to investigate and shape the nature of stellar variability. Such scattered data points in the curves are occurred due to instrumental errors and noise, due to which, it is not possible to accurately classify the nature of stellar variability. To overcome this problem, we adopt the average moving procedure for construction of these diagrams. In this procedure, data points are arranged in increasing order according to their phase values from 0 to 1. In this connection, the average values are determined for sets of five data points such as 1-5, 2-6, 3-7 and so on. This procedure is repeated until we are not computed the average of last remaining five data points. However, a sufficient fraction of the amplitude of light curve also decreases during adoption of this procedure. The resultant phase-folded curves of variables are found to be smooth in comparison of original diagrams. As a result, we conclude that amplitude of stellar pulsation decreases with the increment of smoothness of the phase-folded diagram of variables due to the moving average procedure. In the Figures 8(B) and 9(A), the phase diagrams of variables constructed through the resultant data points as per the average moving procedure.

⁴www.univie.ac.at/tops/Period04

⁵www.home.umk.pl/gmac/SAVS/soft.html

6.2 Structure Index for Stellar Variability

We have computed period of identified variables by two different programs PerSea and PERIOD04. In this connection, we also computed the amplitudes of variables through the visual inspection of phase-folded diagrams as listed in the table 3 and table 4. Since, the amplitudes of identified variables are varied to observational night to night due to observational conditions and aliases frequencies of noise, therefore, we are purposed to a parameter 'Structure index' S_{in} to verify the stellar variability and it is expressed as $S_{in} = A_{phase}/A_{fc}$, where A_{phase} is the amplitude of stellar variability as computed through the resultant phase-folded diagrams. Similarly, A_{fc} is the amplitude of stellar variability as per Lomb-Scorgle periodograms by using PERIOD04. Present analysis indicates that the computed values of structure indexes for variables are independent from the stellar magnitudes, power of periodograms and amplitude of stellar variability. Normalized stellar amplitudes are also independent from the stellar magnitude for similar group of variables. The value of structure index for variables found to be more than one (except $\delta - Scuti$ variables). It indicates that average moving procedure effectively increase smoothness of stellar variability and provides clear shape and characteristics to identify type of their stellar variability.

7 Mean proper Motion and Membership Analysis

7.1 Mean Proper Motion of Core region of NGC 1960

We compared our catalogue with Gaia EDR3 data given by Gaia collaboration et al. (2016, 2021) and found 1579 common stars between them within the studied core region. The distribution of these stars in μ_x - μ_y plane is shown in Fig. 14. The dark filled circles in the figure are those stars that were used to determine the mean proper-motion of the cluster NGC 1960. These stars were identified after excluding those stars which lie outside 3σ deviation from the mean value of proper motion in both RA and DEC directions. After 3σ iteration processes, we have found 1405 stars from which we obtained following mean proper motion in RA and DEC direction of the cluster NGC 1960.

$$\bar{\mu}_x, \bar{\mu}_y = 0.314 \pm 0.026 \text{ mas/yr}, -2.333 \pm 0.037 \text{ mas/yr}$$

The standard deviation values (σ_α , σ_δ) of stellar proper motions of NGC 1960 are found to be 0.996 and 1.402 in RA and DEC respectively. Using these values, the resultant standard deviation $\sigma = \sqrt{\sigma_\alpha^2 + \sigma_\delta^2}$ is estimated

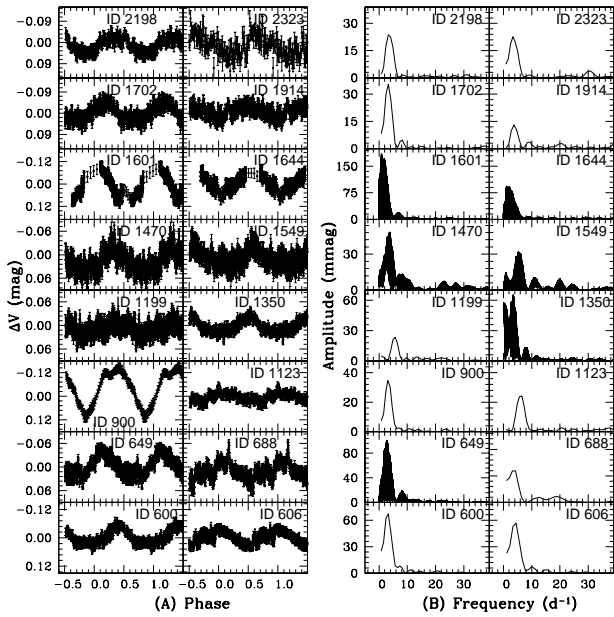


Fig. 11 The left panels represent the phase-folded-diagrams of identified variable stars within the cluster NGC 1960, whereas their corresponding DFT represent in the right panels.

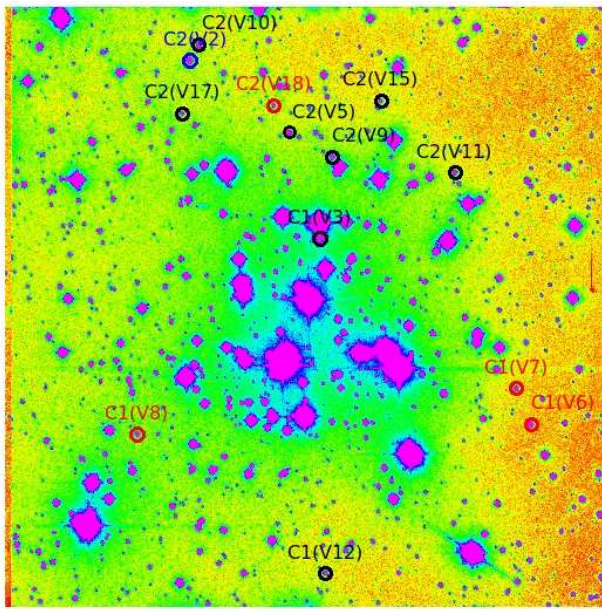


Fig. 12 The finding chart for selected comparison stars within cluster NGC 1960. Identified standard stars are marked by red open circles and they have almost constant brightness/flux during observations. Black open circles represent those long periodic variable stars, for which approximate flux is found for a particular night of observation. However, the value of magnitude is varying night to night.

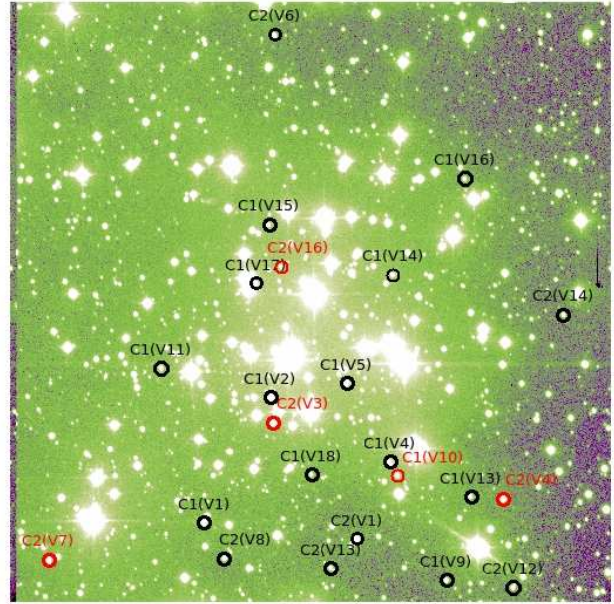


Fig. 13 The finding chart for selected comparison stars within cluster NGC 1960. Red open circles represent those Long term variable stars, for which variation in brightness is also found as daily basis. Black open circles are depicted stars that have irregular flux variation in their light curves as extracted through absolute photometry.

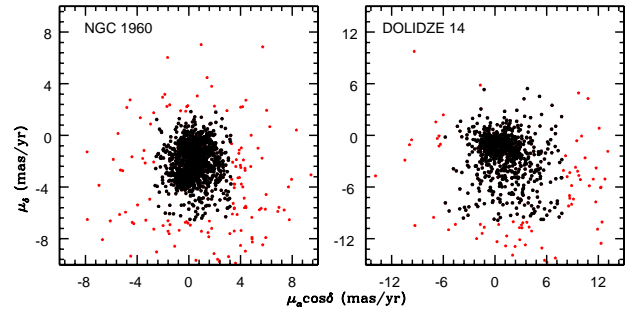


Fig. 14 The distribution of proper motion of stars present in the cluster region. The large points represent those stars which are used to determine the mean proper motion of the cluster.

as 1.734. JO20 has been estimated the mean proper motion of whole cluster of NGC 1960 in *RA* and *DEC* directions as $-0.143 \pm 0.008 \text{ mas yr}^{-1}$ and -3.395 ± 0.008 respectively. These different values indicates that stellar members of this cluster may segregated in inner and outer regions as per their proper motion values.

7.2 Mean Proper Motion of DOLIDZE 14

In the case of DOLIDZE 14, a total of 1137 stars is found within periphery of radius 9.8 *arcmin* at GAIA database. We are found proper motions for 887 stars among them, which are used for computation of mean proper motion of DOLIDZE 14. After 3σ iteration processes, we have found 761 stars from which we obtained following mean proper motion in *RA* and *DEC* direction of the cluster DOLIDZE 14.

$$\bar{\mu}_x, \bar{\mu}_y = 1.050 \pm 0.083 \text{ mas/yr}, -2.254 \pm 0.093 \text{ mas/yr}$$

The estimated standard deviation values ($\sigma_\alpha, \sigma_\delta$) of proper motion values of stars of DOLIDZE 14 are 2.288 and 2.601 in *RA* and *DEC* respectively. These values give resultant standard deviation $\sigma = \sqrt{\sigma_\alpha^2 + \sigma_\delta^2}$ as 3.465.

7.3 Kinematic Probabilities

In the present analysis, those stars are consider to be kinematic members for each cluster, which lie within 3σ limit of the mean proper motion of studied cluster. The proper motion probability is assigned to be 1 for stars having coincident proper motions with the cluster, whereas the proper motion probability is assigned to be 0 for stars having proper motions outside the 3σ limit (Joshi, G.C. 2022). Proper motion probability of stellar members of each cluster is computed as $P_{pm} = 1 - \frac{\sqrt{(\mu_\alpha - \bar{\mu}_\alpha)^2 + (\mu_\delta - \bar{\mu}_\delta)^2}}{3\sigma}$. These values of variable stars of both clusters are listed in sixth column of Table 7.

8 Comparative study of cluster's parameters with variable stars

8.1 Range of Instability strip in the case of NGC 1960

The instability strip is a narrow, almost vertical region in HR diagram, which contains many different type of variable stars. Most stars more massive than Sun enter the instability and become variable at least once after they have left the main sequence (MS)⁶. This strip intersect the MS in the region of A and F stars (have mass

1-2 M_\odot) of studied clusters and extends to G and early K bright super-giants. The common area of instability strip and MS of OCL NGC 1960 seems to be important region (includes A and F stars) to understand the cluster dynamics through the stellar variability and vice-versa. In this connection, the upper and lower limit of region, have A and F stars, are found to be 13.17 *mag* of *V - band* and 16.61 *mag* of *V - band*, respectively and prescribed intercepted region also least affected by the brighter stars and their neighbourhood. As a result, we are carried out time series analysis for finding stellar variability within this magnitude-range. A total of seventeen variables (except V_{18}) of NGC 1960 are identified in this magnitude-range.

8.2 Variable Stars and ZAMS of NGC 1960

By using (*U - B*) vs (*B - V*) Two colour Diagram (TCD), Joshi & Tyagi (2015a) has been determined reddening, $E(B - V) = 0.23 \pm 0.02 \text{ mag}$. JO20 has also computed the reddening, $0.24 \pm 0.02 \text{ mag}$, which is close to previous one. In the present work, the location of variable stars of NGC 1960 has been depicted in (*U - B*) vs (*B - V*) TCD along-with Zero-Age-Main-Sequence (ZAMS) as shown in Figure 15. A ZAMS star has its minimum radius, its maximum mass (for single star evolution), its bluest colour (or hottest effective temperature), and its central core possesses its peak *H/He* (Hanson 1998). After deep inspection of TCD and GAIA database for cluster, author has been drawn following facts:

(1)- Variable stars V_1, V_2, V_3, V_4 are found to be ZAMS stars and have close brightness to each other in *V*-band. The locations of V_1, V_2 and V_4 at the near of bump in (*U - B*) vs (*B - V*) TCD, whereas the location of V_3 is found to be far away these stars. This facts leads different class of V_3 .

(2)- Variable stars $V_8, V_{12}, V_{13}, V_{14}$ and V_{16} are belong to ZAMS of cluster. Variable stars V_8 and V_{12} are member of cluster 1960 and may poses the character of same class of variable stars. Variable stars V_{13}, V_{14} and V_{16} are field stars leads a fact that field stars are also located in just main sequence of cluster.

(3)- Variable stars $V_6, V_{10}, V_{11}, V_{15}, V_{17}$ and V_{18} are not belong to main sequence of cluster and have a confirm membership of cluster.

(4)- Variable stars $V_5, V_7,$ and V_9 neither belong to main sequence of cluster nor have a member of cluster.

8.3 CMDs analysis for NGC 1960

Joshi & Tyagi (2015a) shown the most probable members (MPMs) in (*B - V*) vs *V* Colour Magnitude Diagram (CMD) by comprehensive analysis of photometric, kinematic and spatial probabilistic criteria. These

⁶astronomy.swin.edu.au/cosmos/I/Instability Strips

Table 8 Parallax and distance values of studied variable stars are listed in second and third columns respectively. The stellar proper motion values of R.A. and DEC deirection are given in fourth and fifth columns respectively. The estimated kinematic probabilities of variables are listed in sixth column.

1:- DOLIDZE 14						
Variable ID	Parallax (mas)	Distance (kpc)	Proper Motion in RA (δ)	Proper Motion in DEC (μ)	kinematic Pro. (Old)	kinematic Pro. (GAIA)
V_1	1.2234 ± 0.0162	0.817 ± 0.011	2.317 ± 0.019	-7.763 ± 0.012	--	0.456
V_2	0.7388 ± 0.0772	1.354 ± 0.141	1.903 ± 0.094	1.060 ± 0.054	--	0.671
V_3	0.2453 ± 0.0709	4.077 ± 1.178	0.590 ± 0.077	-0.856 ± 0.046	--	0.858
V_4	0.9287 ± 0.1791	1.077 ± 0.208	-1.934 ± 0.204	-3.928 ± 0.116	--	0.671

2:- NGC 1960						
Variable ID	Parallax (mas)	Distance (kpc)	Proper Motion in RA (δ)	Proper Motion in DEC (μ)	kinematic Pro. (Old)	kinematic Pro. (GAIA)
V_1	0.8858 ± 0.0188	1.129 ± 0.024	-0.204 ± 0.023	-3.406 ± 0.016	0.40	0.771
V_2	0.8430 ± 0.0180	1.186 ± 0.025	-0.011 ± 0.023	-3.506 ± 0.017	0.35	0.766
V_3	2.9243 ± 0.0228	0.342 ± 0.003	-3.018 ± 0.027	-4.932 ± 0.019	0.06	0.188
V_4	0.8382 ± 0.0194	1.193 ± 0.027	-0.432 ± 0.024	-3.219 ± 0.017	0.99	0.777
V_5	0.2889 ± 0.0255	3.461 ± 0.305	0.675 ± 0.028	-2.292 ± 0.021	0.05	0.930
V_6	0.8543 ± 0.0254	1.171 ± 0.035	-0.209 ± 0.034	-3.440 ± 0.023	0.81	0.765
V_7	0.1985 ± 0.0275	5.038 ± 0.698	0.113 ± 0.027	-1.594 ± 0.021	0.00	0.853
V_8	0.8206 ± 0.0350	1.219 ± 0.052	-0.042 ± 0.040	-3.525 ± 0.026	0.79	0.761
V_9	0.4966 ± 0.0857	2.014 ± 0.348	0.010 ± 0.097	-3.579 ± 0.072	0.91	0.753
V_{10}	0.8022 ± 0.0309	1.246 ± 0.048	-0.244 ± 0.036	-3.276 ± 0.027	0.04	0.789
V_{11}	0.8130 ± 0.0350	1.230 ± 0.053	-0.401 ± 0.043	-3.543 ± 0.030	0.94	0.730
V_{12}	0.9063 ± 0.0400	1.103 ± 0.049	-0.059 ± 0.049	-3.355 ± 0.035	0.00	0.791
V_{13}	0.4407 ± 0.0366	2.269 ± 0.188	0.723 ± 0.041	-3.327 ± 0.029	0.00	0.793
V_{14}	0.0995 ± 0.1441	10.050 ± 14.555	0.692 ± 0.159	-2.518 ± 0.128	0.99	0.919
V_{15}	0.9037 ± 0.0496	1.106 ± 0.061	-0.331 ± 0.055	-3.593 ± 0.037	0.00	0.728
V_{16}	1.1574 ± 0.0478	0.864 ± 0.036	4.521 ± 0.057	-1.697 ± 0.038	0.93	0.182
V_{17}	0.9037 ± 0.0448	1.107 ± 0.055	-0.178 ± 0.055	-3.418 ± 0.040	0.52	0.771
V_{18}	0.8396 ± 0.0460	1.191 ± 0.065	-0.246 ± 0.054	-3.425 ± 0.039	0.95	0.764

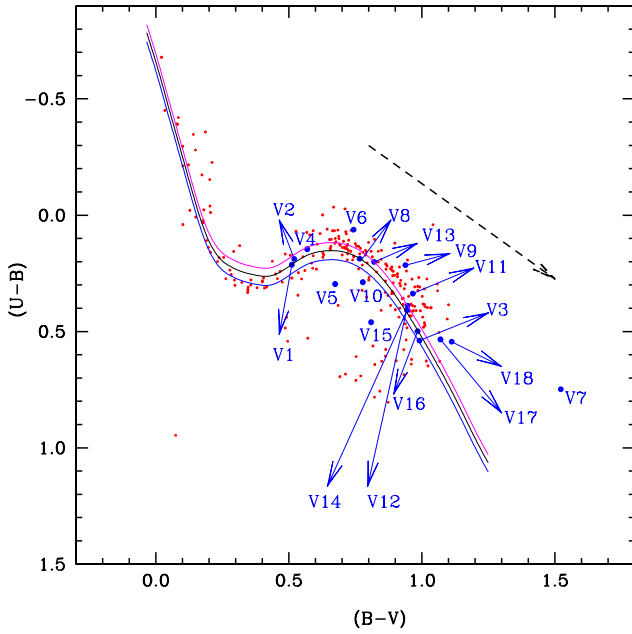


Fig. 15 $(B - V)$ vs $(U - B)$ colour-colour diagram for the MPMs in the field of cluster NGC 1960 as per Joshi & Tyagi (2015). For clarity, variable stars of NGC 1960 are represented by blue dots. The dotted black arrow shows a slope of normal reddening vector $E(U - B)/E(B - V) = 0.72$. The solid black line shows the best fit taken in account of 0.23 and 0.17 mag shift in $(B - V)$ and $(U - B)$, respectively while pink and blue lines represent an error of ± 0.15 in the reddening vector respectively.

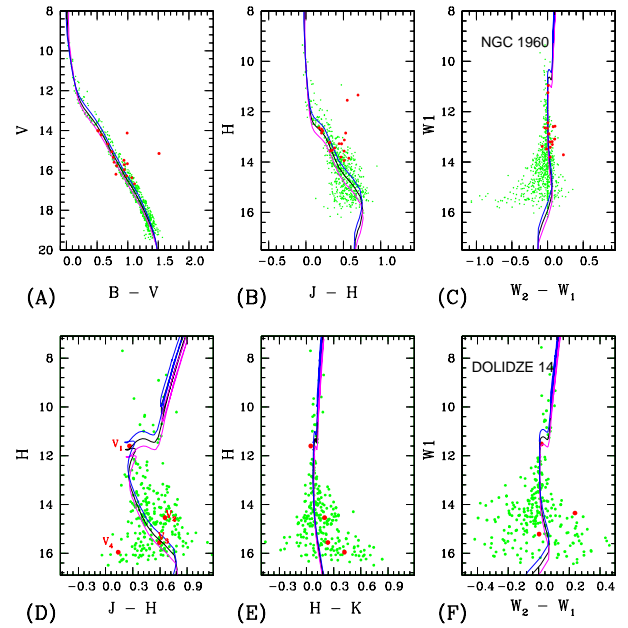


Fig. 16 The upper and bottom panels of this figure represent CMDs for NGC 1960 and DOLIDZE 14, respectively. The blue dots on each panel represent the variable stars as identified by us through the time series photometric data while red dots represent the probable members of the studied clusters as extracted from the work of Joshi & Tyagi (2015) and Joshi & Tyagi (2015b). The black solid lines represent the best fitted theoretical isochrones as given in the previous studies.

MPMs are found along with MS of NGC 1960 and also well aligned with a well fitted theoretical isochrone as depicted in upper panels of Figure 16. The pink line of each CMD represents the well fitted theoretical as computed by Joshi & Tyagi (2015a). In the $(J - H)$ vs H CMD, author did not find stellar alignment by MPMs along with theoretical isochrone for H-magnitude range of 12.5-13.2 *mag* as shown in Figure 16(B). It leads a correction in an estimation of distance-modulus. Author overplot Marigo's theoretical isochrones on the CMDs by varying the distance modulus and age simultaneously by keeping reddening $E(B - V) = 0.23$ mag. From the best visual isochrone fit to the varying age and distance combinations, author obtained a distance modulus $(V - M_V) = 11.05 \pm 0.030$ mag and $\log(\text{Age}) = 7.35 \pm 0.05$ (yr) for cluster NGC 1960. Employing the correction for the reddening and assuming a normal reddening law, this corresponds to a true distance modulus $(m - M)_0 = 10.34 \pm 0.30$ mag or a distance of 1.169 ± 0.173 kpc for the cluster. The computed value of distance modulus is utilized to identify the true member of cluster as per retrieved value of distance/parallax value of individual star.

The best fitted theoretical isochrones in each CMD is represented by black line and identified variable stars are depicted by red dots. Variable stars V_3 and V_7 shows colour excess in near-infrared bands, however these stars also found along-with the theoretical isochrone in $W_2 - W_1$ vs W_1 CMD as depicted in Figure 16(C).

8.4 CMDs analysis for DOLIDZE 14

In the case of DOLIDZE 14, there are no saturated brighter star of unresolved center. As a result, author did not need employ any selection criteria of stellar magnitudes to identify variable stars for this cluster. The red dots of lower panels of Figure 16 represent identified variable stars for DOLIDZE 14. The distance modulus and distance for cluster DOLIDZE 14 has been estimated by ? as 11.12 ± 0.18 mag and 1.67 ± 0.14 kpc respectively. In this connection, the best fitted isochrone is depicted by black solid line in Figure 16, whereas pink and blue lines represent lower and upper limits for apparent distance modulus. The distance of identified variable stars of this cluster are listed in table 8. Variable star V_2 is close to cluster periphery, whereas variable star V_4 seems to be confirmed member of cluster. Other two variable stars V_1 and V_3 are not belong to cluster as per known parameters.

9 Detected Variables in DOLIDZE 14

The time series observation of this cluster has been taken in Near-Infrared region by using I-band with ef-

fective wavelength 8000 \AA . In the present analysis, a total of 4 variable stars are found in the observed field of DOLIDZE 14.

9.1 Miscellaneous type variable star

Some periodic stars could not be classified in any particular class of variable stars as per their estimated parameters and phased light curves.

9.1.1 Star IDs 004 (V_1), 005 and 006 of DOLIDZE 14

As par 'PERIOD04' and 'PerSea' code analysis, the period values of V_1 are found to be 0.0599 ± 0.0067 d and 0.0606 ± 0.0068 respectively. Its individual distance value (0.817 ± 0.011) is very far away from the cluster distance. Its least kinematic probabilistic value also supports that it is not a member of cluster. Thus, it can not be classified as a main sequence star for the studied cluster. Potential variable V_1 is located just near the turn off point of CMD with blue colour. As per analysis of properties of this star, it seems to be a miscellaneous type variable star.

Light curve of this variable has been compared with the light curves of star IDs 005 ($4^h : 06^m : 26.85^s$, $+27^0 : 18' : 24.2''$) and 006 ($4^h : 06^m : 43.39^s$, $+27^0 : 17' : 46.9''$). Light curves of selected comparison stars do not show any sign of periodic variability.

9.2 Potential Rotational Variable star

Rotational variable stars have a change in apparent brightness due to large spots on their surfaces. The light curves of such type variable stars are typically very noisy due to evolution of star spots over time.

9.2.1 Star IDs 085, 086 and 088 (V_2) of DOLIDZE 14

A value of period for variable star V_2 has been calculated to be 0.0939 ± 0.0195 d and 0.0714 ± 0.0074 by the code of 'PERIOD04' and 'PerSea' respectively. Its amplitude, distance and kinematic membership for cluster is computed to be 0.088 mag, 1.354 ± 0.141 kpc and 0.671 respectively. Its location in $(J - H)$ vs H CMD has found towards red colour as depicted in Figure 16. As a result, this star seems similar to a rotational type star. As DOLIDZE 14 is an old cluster having an age of about 1.26 ± 0.08 Gyr, it is rare/ impossible that any star in the cluster are found to be rotational variables. In this connection, this variable star can not have a member of cluster.

In Figure 10, the comparative Light curves of star IDs 085 ($4^h : 07^m : 02.90^s$, $+27^0 : 15' : 53.4''$) and 086

($4^h : 06^m : 38.14^s$, $+ 27^0 : 22' : 33.0''$) along with variable star V_2 has been depicted. Author did not find any sign of periodic variability in the light curves of said comparison stars.

9.3 Potential Binary system of stars

A sudden drop in brightness of binary system finds due to eclipse and transit of its component stars during their orbit along plane of our line of sight.

9.3.1 Star IDs 109, 110 (V_3) and 111 of DOLIDZE 14

Variable star V_3 poses a deep of Flux in its light curve and this feature is similar to binary system. Due to lack of time series observation of studied cluster, author found drop in intensity only once. The computed period is $0.1349 \pm 0.0359 d$ and close to observation session for DOLIDZE 14 and leads a dubious analysis. Its distance is found to be $4.077 \pm 1.178 kpc$ and leads it is as a non-member of cluster. As a result, variable star V_3 may be a system of binary stars with unknown periodic eclipse.

Light curves of comparison star IDs 109 ($4^h : 06^m : 42.69^s$, $+ 27^0 : 20' : 30.2''$) and 111 ($4^h : 06^m : 45.90^s$, $+ 27^0 : 17' : 00.8''$) have no sign of stellar variability as depicted in Figure 10.

9.3.2 Star IDs 183, 184 (V_4) and 185 of DOLIDZE 14

Variable star V_4 is not found to be a member of of DOLIDZE 14 as per its distance $1.077 \pm 0.208 kpc$ and membership probability 0.671. By using the codes of 'PERIOD04' and 'PerSea', the period of this variable star is computed as $0.0674 \pm 0.0085 d$ and $0.0714 \pm 0.0062 d$ respectively. Its light curve poses character of binary stars as depicted in Figure 10.

Light curves of comparison star IDs 183 ($4^h : 06^m : 24.45^s$, $+ 27^0 : 14' : 24.9''$) and 185 ($4^h : 07^m : 02.11^s$, $+ 27^0 : 17' : 52.8''$) are shown the more variation in brightness compare with other comparison stars of studied cluster. However, there are no periodic variation in comparative light curve of comparison stars (Star IDs 183 and 185) and have low variation of brightness compare to their comparative light curves with variable star V_4 .

10 Detected Variables in NGC 1960

In this paper, eighteen variables were detected in the observed field of NGC 1960, among them only four variable stars are common with JO20. According to the

behavior of the light curves and the period analysis, classification of detected variables were made. Among the eighteen detected variables of NGC 1960, one as EB, one as planet transit, one as $\gamma - Dor$, two as $\delta Scuti - \gamma - Dor$, two as LADS, two as irregular, two as rotational, three as RRC and four as Ellipsoidal type variable stars.

10.1 $\gamma - Doradus$ variables

A multiperiodic stars with g-mode pulsation is known to be $\gamma - Doradus$. These are typically young, early F- or late A-type main stars with periods in the range of about $0.3 - 3 d$ and brightness fluctuation $\sim 0.1 mag$ Balona et al. (2011).

10.1.1 Star ID 606 (V_2), 616 and 626 of NGC 1960)

In the case of variable star ID 606, star IDs 616 ($5^h : 36^m : 26.45^s$, $+ 34^0 : 07' : 39.3''$) and ID 624 ($5^h : 35^m : 50.83^s$, $+ 34^0 : 06' : 03.6''$) are selected for comparing their light curves with it. JO20 is assigned ID 606 as cluster member $\delta - Scuti$ variable star with period $0.27632 \pm 0.00008 d$ and it is denoted by V_{35} in their analysis. In the present work, its period is computed by the code of 'PERIOD04' and 'PerSea' as $0.2246 \pm 0.0599 d$ and $0.6250 \pm 0.0274 d$, respectively. Since its light curves in Figure 4 are not showing any indication of period value below 7.6 hours, therefore its period value via Anova analysis is seems to be more accurate. Thus, Star ID 606 is found to be $\gamma - Doradus$ variable star instead of $\delta - Scuti$. Its kinematic probability makes it as most probabilistic member of cluster.

The light curves of ID 616 are showing irregular flux variations, whereas light curves of ID 624 have a characteristics of long periodic variables. Almost constant magnitude found for ID 624 during 7-8 hours observations.

10.2 $\delta - Scuti - \gamma - Doradus$ hybrid variables

Generally, $\gamma - Doradus$ instability strip is found to be below the $\delta - Scuti$ strip. Some portion of instability strips of both these classes is overlap to each other. Such hybrid candidates are already reported in open clusters by Hartman et al. (2008) and Joshi et al. (2020).

10.2.1 Star IDs 592, 595 and 600 (V_1) of NGC 1960

Author has selected two stars, ID 592 ($5^h : 36^m : 39.44^s$, $+ 34^0 : 06' : 12.3''$) and ID 595 ($5^h : 36^m : 41.27^s$, $+ 34^0 : 09' : 29.9''$), for comparing their light

curves with Star ID 600 and these stars are marked by C1(V1) and C2(V2) in Figure 13. Joshi et al. (2020) has assigned ID 595 as a cluster member and a hybrid δ Scuti γ Doradus variable star and it is marked by V_{27} in their analysis. All of these stars have minimum in V-magnitude and colour (B-V) as listed in Table 5. After inspection of light curves of Star IDs 592 and 595 in Figure 4, author noted that both stars have shown approximate similar pattern. The light curves of ID 595 have regular pattern of flux variation with very low amplitude and author considered it as an effect of instrumental pseudo-variability. Light curves of star ID 600 have shown prominent variation in its magnitude. The value of its period is found to be $0.3057 \pm 0.0815 d$ and $0.4000 \pm 0.1055 d$ by code of 'PERIOD04' and 'PerSea', respectively. It may be a δ Scuti – γ Doradus star. Its location within cluster is shown in Figure 2 by mark M36(V1). It is also found more kinematic probabilistic member of cluster by the author.

10.2.2 Star IDs 678, 688 (V_4) and 694 of NGC 1960)

Star IDs 678 ($5^h : 36^m : 33.38^s$, $+34^0 : 10' : 13.0''$) and 694 ($5^h : 36^m : 37.21^s$, $+34^0 : 12' : 39.3''$) are selected as possible comparison star. These stars are marked by C1(V1) and C2(V2) in Figure 13 and their physical coordinates are found closest compare than other set of stars. Variable star V_4 is assigned to be a γ Doradus variable star with period $1.07066 d$ and marked by V_{62} in the work of Joshi et al. (2020). In the present analysis, its period is found to be $0.3115 \pm 0.1168 d$ by the code of 'PERIOD04', whereas the said value is 0.2857 ± 0.0706 by the ANOVA analysis as per code of 'PerSea'. It is more kinematic probabilistic member of cluster and marked by M36(V4) in Figure 2.

The trend of light curves of Star IDs 678 and 694 are approximately similar to each other. However, light curves of star ID 694 shows a regular feature of short periodic variability and it is considered to be pseudo-variability by author.

10.3 RR Lyre stars

Over 80 % of all variables known in globular clusters are RR Lyre stars (Clement et al. 2001). One d-type RR Lyre variable star in the open cluster NGC 2141 has been reported by Luo (2015). RR Lyrae variables do not follow a strict period-luminosity relationship at visual wavelengths, although they do in the infrared K-band (Catelan et al. 2004).

10.3.1 Star IDs 635, 645 and 649 (V_3) of NGC 1960

Variable star V_3 shows a peculiar phase-fold diagram with slowly descending and quick ascending branches

as similar to the RR Lyre variable stars. The codes of 'PERIOD04' and 'PerSea' provide its period value as $0.3598 \pm 0.0001 d$ and $0.4000 \pm 0.2086 d$ respectively. The precise value of period is too long for normal δ Scuti star and its position in ($U-B$) vs ($V-B$) TCD is found to be far away from the group of identified δ – Scuti variable stars. However, its position in ($B-V$) vs V CMD and ($U-B$) vs ($V-B$) TCD is just on the main sequence. In this connection, its least kinematic probabilistic value and distance indicate that it is not a member of cluster NGC 1960. Thus, It is likely a RR Lyre d variable star.

In the case of this variable star, Star IDs 635 ($5^h : 36^m : 09.47^s$, $+34^0 : 08' : 51.2''$) and 645 ($5^h : 36^m : 29.11^s$, $+34^0 : 07' : 42.2''$) are selected for the comparative analysis. Star ID 635 is assigned to be γ – Dor variable star by JO20. In this connection, author found that light curves of Star ID 635 shows characteristic similarities that of star ID 624. Similarly, light curves of star IDs 616 and 645 have similar characteristics. Thus, the nature of light curves of star IDs 616, 624, 635 and 645 is either uncertain in nature or some kind of irregular variability.

10.3.2 Star IDs 1431, 1470 (V_9) and 1484 of NGC 1960

The variable star V_9 is assigned to be rotational variable star, main sequence star and cluster member by JO20 and marked by V_{48} in their analysis. Its period is computed to be $0.2667 \pm 0.0006 d$ and $0.4629 \pm 0.0399 d$ by code of 'PERIOD04' and 'PerSea' respectively. These codes clearly provide two distinct values of period. Its location in ($U-B$) vs ($V-B$) TCD indicates that it does not fulfill the criteria of ZAMS within errors as depicted in Figure 15. Its distance is $2.014 \pm 0.348 kpc$ as per GAIA database, which is very far away from the cluster NGC1960. Thus, variable star V_9 neither main sequence star nor a member of cluster NGC 1960. Its highest probabilistic values are just coincidence with members of cluster. Since, its characteristics are not well matched with rotational type variable star, therefore author switched off its previous classification as did by JO20.

The slowly descending and quick ascending nature of its phase-folded curve indicate that variable star V_9 is a RR Lyre star.

Star IDs 1431 ($5^h : 36^m : 45.65^s$, $+34^0 : 11' : 25.0''$) and 1484 ($5^h : 36^m : 00.93^s$, $+34^0 : 09' : 07.7''$) has selected comparison stars for variable star v_9 . Their locations in 13 and 12 are marked by C1(V9) and C2(V9) respectively. As per visual inspection, author found these comparison stars are far away from the variable star V_9 . The comparative light curves of star IDs

1431 and ID 1484 show a constant magnitude difference during entire observational session. As per GAIA database, The parallax value for Star Ids 1431 and 1484 is 0.6473 mas and 0.2435 mas , respectively. The colour-difference $(B - V)_0$ for both comparison stars is greater than 1.0 mag. Such pair of comparison stars is not possible for any given variable star as per differential photometry. As a result, magnitude variation of stars is free from stellar distance and colour-difference in absolute/ standard photometry. However, author found some amount of magnitude variation for both comparison stars, but it seems to be impact of instrumental nature due to their constant magnitude difference.

10.3.3 Star IDs 2323 (V_{16}), 2352 and 2379 of NGC 1960

As per the codes of 'PERIOD04' and 'PerSea', the estimated values of period for V_{16} are $0.3005 \pm 0.0801 \text{ d}$ and $0.2941 \pm 0.0171 \text{ d}$ respectively. Its distance has given to be $0.864 \pm 0.036 \text{ kpc}$ in GAIA database and it is close to us with respect to the cluster NGC 1960. In this connection, its least kinematic probabilistic value (as per GAIA database) also confirms it as Field Star. Although, its position in $(U - B)$ vs $(V - B)$ TCD is just on the main sequence as depicted in Figure 15. Its phase curve posses a character of asymmetrical magnitude variation with increasing rapidly and decreasing slowly, like as Lyre variable stars. Its phase curve is depicted in Figure 11.

Author has selected two stars, ID 2352 ($5^h : 36^m : 03.82^s, + 34^0 : 11' : 51.5''$) and ID 2379 ($5^h : 36^m : 12.86^s, + 34^0 : 07' : 54.1''$), for comparing their light curves with that of variable star V_{16} . Both stars are showing approximate constant magnitude difference during entire observation sessions. However, their light curves have character of Long Periodic Variables, but seems to be instrumental effect. As per observations of each individual night, they have low magnitude variation compare to variable star V_{16} as depicted in upper panels of Figure 9. The pixel distances of these stars (IDs 2323, 2352, 2379) indicate that they are far away to each other. Colour, $(B - V)_0$, values of V_{16} and ID 2352 are close to each other, but far away from that of ID 2379. Thus, similar character of light curves for ID 2352 and ID 2379 confirms colour- free selection of comparison stars during time series analysis via absolute photometry.

10.4 Eclipsing Binaries type Variable Stars

Eclipsing binaries are easily classified into two main groups: detached system or semidetached (Balona et

al. 2015). Spherical or slightly ellipsoidal components are found in detached system (Algol type, EA), whereas tidally distorted stars are present in semidetached system (β Lyre System, EB). The light remains almost constant between eclipses of EA systems. Between eclipses, a continuous change of the combined brightness is found for EB system, leads impossibility to specify the exact times of onset and end of eclipses. Stars with planets may also show flux variations if associated planets for any star pass between Earth and the star.

10.4.1 Star IDs 900 (V_5), 902 and 904 of NGC 1960

It is marked by V_{55} by JO20 and it is assigned to be field star in their analysis. In addition, they found a minima in its phase curve with amplitude of 218 mmag . Author also found only one minima in its light curves. As a result, the eclipse of variable star V_5 occurs due to a giant planet instead of second companion star. In the present work, the light curves of variable star V_5 are depicted in Figure 5. The full phase of planet transit is found in the extracted light curve at 20 December 2013 and a portion of this planet transit also detected in the extracted light curve at 12 January 2015. The gap of both detected transit events is computed to be 01 year 23 days 3 hours. The time of planet transit is computed to be $0.3182 \pm 0.0848 \text{ d}$ and $0.2857 \pm 0.0454 \text{ d}$ through the codes of 'PERIOD04' and 'PerSea' respectively. These both values are equivalent to that observational session, in which transit epoch has detected. The amplitude of transit epoch is found up to 248 mmag . After visual inspection of light curves of this variable, estimated time of planet transit is approximately $0.216 \pm 0.018 \text{ d}$. Its distance is $3.461 \pm 0.305 \text{ kpc}$ and far away from the cluster periphery. Thus, it is a background field star in the field of cluster NGC 1960.

Light curves of Star IDs 902 ($5^h : 36^m : 25.02^s, 34^0 : 09' : 17.5''$) and 904 ($5^h : 35^m : 58.41^s, 34^0 : 08' : 11.8''$) are selected for comparative analysis with variable star V_9 . Both comparison stars have nearby colour, $((B - V)_0)$, value with variable star V_9 . Light curves of Star ID 904 contain the short periodic variation with low amplitude, whereas light curves of star ID 2 have irregular variation of brightness. Since, their comparative light curves have almost constant value of brightness fluctuation, therefore, fluctuation of their light curves is a result of instrumental errors in nature.

10.4.2 Star IDs 1576, 1601 (V_{11}), 1613 of NGC 1960

Based on 'PERIOD04' and 'PerSea' code analysis, author obtained period value for V_{11} as $1.1053 \pm 0.0007 \text{ d}$ and $1.0980 \pm 0.1033 \text{ d}$, respectively. Its distance is

1.230 ± 0.053 kpc from us and its kinematic probability of membership in cluster is estimated to be 0.73 as per GAIA database. Thus, variable star V_{11} is a member of cluster. It is easily seen in its light curves, which are depicted in Figure 7 that short periodic variations are superimposed with its principal period. It becomes difficult to specify exact time of onset and end of eclipses of companion stars due to their continuous change of brightness and its phase-folded diagram shows superimposed character of both eclipses as depicted in Figure 11. As a result, this star is classified as semidetached eclipsing binary (EB) type variable star.

The pattern of brightness variation in light curves for star ID 1576 ($5^h : 36^m : 23.38^s$, $34^\circ : 05' : 18.1''$) is similar to variable star V_{11} as depicted in Figure 7. As a result, author concludes that star ID 1576 is also a EB star with low amplitude. During the observational session of each night, light curves of star ID 1613 ($5^h : 36^m : 02.64^s$, $34^\circ : 11' : 46.0''$) shows incremental slop over time with less inclination. In this connection, the fluctuation of its light curves is seems to be instrumental errors in nature.

10.5 Ellipsoidal Variable stars

In the periodogram of an ellipsoidal binary, sharp peaks are found at the fundamental frequency and its harmonics. Usually only the first harmonic is visible and the amplitude of fundamental frequency is less than first harmonic in some cases. As a consequence of differences in harmonic content, the shapes of the light curves can be very different (Balona et al. 2015). These stars are close binary system and tidally distorted components. There are no eclipses in these variables due to the low inclination of the orbital axis, but the changing aspect towards us causes a change in brightness. Such brightness variation are a combination of tidal distortion, reflection and beaming. The period of the reflection and beaming contributions is the same as the orbital period whereas the ellipsoidal effect has half the orbital period (Balona et al. 2015).

10.5.1 Star IDs 1123 (V_6), 1124 and 1130 of NGC 1960

Based on the codes of 'PERIOD04' and 'PerSea', the period of V_6 is found to be 0.1528 ± 0.0194 d and 0.1538 ± 0.0369 d, respectively. Its distance (1.171 ± 0.035 kpc) and kinematic probabilistic value (0.765) indicate that it is a member of cluster. Since, non-sinusoidal variation is found in its phase folded light curve, therefore it contains character of ellipsoidal type variable star. However, comprehensive analysis of its light curves during whole observational session indicates that it is an

irregular type variable. As a result, it is classified as an irregular variable with character of ellipsoidal.

Star ID 1124 ($5^h : 36^m : 28.92^s$, $34^\circ : 13' : 23.2''$) is selected as first comparison star for variable star V_6 . It shows almost constant magnitude over time as shown in Figure 5. Thus, it is classified as standard star in the direction of cluster NGC 1960 and its physical location is marked by C1(V_6) in Figure 12.

Similarly, star ID 1130 ($5^h : 35^m : 48.78^s$, $34^\circ : 07' : 46.3''$) is selected as second comparison star for variable star V_6 . This star is classified as irregular type variable by JO20 and marked by V_{70} in their analysis. After visual inspection of its light curves in Figure 5, author also confirms its character of irregular type variable star.

10.5.2 Star ID 1197, 1199 (V_7), 1204 of NGC 1960

The value of period for variable star V_7 is computed to be 0.1747 ± 0.0254 d and 0.1695 ± 0.0154 d by using codes of 'PERIOD04' and 'PerSea' respectively. In the present work, its kinematic probabilistic value is estimated to be 0.853 as per GAIA database. Unfortunately, its distance (5.038 ± 0.698 kpc) does not confirm its membership for a member of cluster. Due to a non-sinusoidal variation of brightness in its light curves, variable star V_7 is classified as ellipsoidal type variable. Its position in ($U - B$) vs ($B - V$) TCD confirms its redder character.

Its First Comparison star, ID 1197 ($5^h : 36^m : 25.21^s$, $34^\circ : 13' : 04.1''$), shows constant magnitude during observational session as depicted in Figure 6. As a result, it is a standard star and its position is marked by C1(V_7) in Figure 12.

Similarly, light curves of its second comparison star, ID 1204 ($5^h : 36^m : 43.20^s$, $34^\circ : 02' : 51.6''$), show the character of irregular type variable.

10.5.3 Star IDs 1701, 1702 (V_{13}) and 1732 of NGC 1960

A value of distance for variable star, V_{13} , is 2.269 ± 0.188 kpc as per GAIA database. Its kinematic probabilistic value shows just coincide with the member of cluster. As per codes of 'PERIOD04' and 'PerSea', the estimated value of period for variable star V_{13} is 0.3057 ± 0.0815 d and 0.2857 ± 0.0762 d, respectively. Due to a non-sinusoidal variation of brightness in its light curves as depicted in Figure 8, it is classified as ellipsoidal type variable star. Star IDs 1701 ($5^h : 36^m : 36.95^s$, $34^\circ : 11' : 57.0''$) and 1732 ($5^h : 36^m : 44.29^s$, $34^\circ : 08' : 55.9''$) are selected for comparative analysis and their positions are marked by C1(V_{13}) and C2(V_{13}) in Figure 13. After visual inspection of light curves of both comparison

stars in Figure 8, author found a constant magnitude difference for both comparison stars. As a result, it is concluded that character of irregular type variable of both stars is an instrumental effect in nature.

10.5.4 Star IDs 1893, 1914 (V_{14}) and 1915 of NGC 1960

As per codes of 'PERIOD04' and 'PerSea', estimated value of period for variable star V_{14} is computed to be $0.2665 \pm 0.0711 d$ and $0.2222 \pm 0.0775 d$, respectively. It is located $10.050 \pm 14.555 kpc$ as per GAIA database, which is highly uncertain. Only highly kinematic probabilistic value does not enough to assign membership status for any stars as we found in previous discussion. Its depicted light curves in Figure 8 show a non-sinusoidal variation of brightness leads it is as ellipsoidal type variable star. Its location in $(U - B)$ vs $(B - V)$ TCD is just on the main sequence.

Star IDs 1893 ($5^h : 36^m : 13.78^s$, $34^\circ : 10' : 18.2''$) and 1915 ($5^h : 36^m : 18.07^s$, $34^\circ : 13' : 58.4''$) in Figure 13 are marked by C1(V_{14}) and C2(V_{14}) respectively. Light curves of Star ID 1893 show character of long periodic variables, whereas Light curves of star ID 1915 are almost constant for some night of observation and have incremental slope with low inclination for other nights of observation.

10.6 Rotational Variable

Stellar rotation and magnetic activity are normally associated with a main-sequence star of G or later spectral type (Joshi et al. 2020). Amplitude of pulsation of these stars have typically less than 0.1 mag. Thus, these stars are characterized by small amplitude, and red in colour $(B - V)_0 > 0.5 mag$. Periods of rotational variable stars can widely vary due to its tied with the rotation of the stars themselves.

10.6.1 Star IDs 1345, 1348 and 1350 (V_8) of NGC 1960

By Using codes of 'PERIOD04' and 'PerSea', the value of period for V_8 is estimated to be $0.2864 \pm 0.0007 d$ and $0.2857 \pm 0.0947 d$ respectively. It is located at $1.219 \pm 0.052 kpc$ from us and this value is close with the distance of cluster. In this connection, its kinematic probabilistic value for cluster membership is 0.761 leads a member of studied cluster. It is red in colour, $(B - V)_0 = 0.766 mag$. Its location in $(U - B)$ vs $(B - V)$ TCD is found along with ZAMS as depicted in Figure 15. All the above characters make it a rotational type variable star.

Light curves of star IDs 1348 ($5^h : 36^m : 29.70^s$, $34^\circ :$

$04' : 53.6''$) and 1345 ($5^h : 36^m : 43.22^s$, $34^\circ : 06' : 38.6''$) are depicted in Figure 6. Almost constant magnitude in light curves of star ID 138 make it a standard star, whereas star ID 1345 contains a character of long periodic type variable stars.

10.6.2 Star IDs 1644 (V_{12}), 1732 and 1734 of NGC 1960

Based on 'PERIOD04' and 'PerSea' code analysis, obtained value of period for variable star V_{12} is $0.8538 \pm 0.0004 d$ and 0.6667 ± 1.0505 respectively. In $(U - B)$ vs $(B - V)$ TCD, it is just located on the main sequence. It contains redder character in colour, $(B - V)_0 = 0.946 mag$. As per GAIA database, its distance is found to be $1.103 \pm 0.049 kpc$ with kinematic probability 0.791. Thus, it is a member of studied cluster with main sequence. Amplitude of this variable is found to be 94 *mmag* via code of PERIOD04. In this connection, it is classified as rotational type variable star.

Light curves of star ID 1732 ($5^h : 36^m : 44.29^s$, $34^\circ : 08' : 55.9''$) shows short term variability with low amplitude, which seems to be instrumental error in nature. Beside this, it is approximately constant magnitude during observation. Other hand, Light curves of star ID 1734 ($5^h : 36^m : 46.46^s$, $34^\circ : 12' : 51.3''$) show an incremental slope of low inclination over observation as depicted in Figure 7.

10.7 Low Amplitude Delta Scuti Variable

Low-amplitude delta Scuti stars (LADS) contains pulsation with smaller amplitudes. The low-amplitude stars can be pre-main, main or post-main sequence stars, and may either be multiperiodic or monopерiodic ⁷.

10.7.1 Star IDs 1549 (V_{10}), 1553 and 1569 of NGC 1960

The value of distance ($1.246 \pm 0.048 kpc$) and kinematic probability (0.789) of variable star V_{10} confirms its membership of the cluster. Its location in $(U - B)$ vs $(B - V)$ TCD makes it as a post-main sequence star. Author analyzed the frequencies of variable star V_{10} with Fourier and variance analysis by using codes of 'PERIOD04' and 'PerSea'. After these analyses, the computed period is found to be $P_1 = 0.1886 \pm 0.0003$ and $P_2 = 0.2404 \pm 0.0226$, respectively, leads $P_1/P_2 = 0.78$. Amplitude of pulsation is 74 *mmmag* as per

⁷aavso.org/vsots_delsct

Lomb-Scargle algorithm. So it is suggested that V_{10} is a multi-periodic $\delta - Scuti$ star with low amplitude. Due to almost constant difference of stellar magnitudes in comparative light curves of Star IDs 1553 ($5^h : 36^m : 34.70^s$, $34^\circ : 10' : 22.7''$) and 1569 ($5^h : 35^m : 49.15^s$, $34^\circ : 06' : 15.1''$), their magnitude variation for an observational night is a result of instrumental transformation. However, light curves of star ID 1569 show a character of long-term variability as shown in Figure 7.

10.7.2 Star IDs 2195, 2198 (V_{15}) and 2222 of NGC 1960

The variable star (V_{15}) is a member of cluster due to its distance (1.106 ± 0.061 kpc) and kinematic probability (0.728). It is also found a post-main sequence star as its position in ($U - B$) vs ($B - V$) TCD. The value of period for variable star V_{15} is computed to be 0.3039 ± 0.0810 d and 0.2041 ± 0.0105 d by using the codes of 'PERIOD04' and 'PerSea', respectively and leads to $\nu_1 : \nu_2 = 3 : 2$. As per Lomb-Scargle algorithm, pulsation amplitude is 72 mmag for this star. Thus, it is found to be multi-periodic low amplitude $\delta - Scuti$ variable star.

There are no sign of reasonable variability in the light curves of star IDs 2195 ($5^h : 36^m : 08.50^s$, $34^\circ : 07' : 37.9''$) and 2222 ($5^h : 35^m : 55.14^s$, $34^\circ : 10' : 10.8''$) and their comparative light curves show almost constant difference for their magnitudes as depicted in Figure 8.

10.8 Irregular Variable Stars

The variations in brightness show no regular periodicity in an irregular type variable star. Such stars are divided into eruptive and irregular pulsating variable stars. The variation of brightness of an eruptive variable star happens due to violent processes and flares occurring in its chromosphere and corona. Eruptive variable stars are found near the main sequence.

10.8.1 Star IDs 2439, 2451 (V_{17}) and 2479 of NGC 1960

The values of distance and kinematic probability for variable star V_{17} are found to be 1.107 ± 0.055 kpc and 0.771 respectively. As a result, it is assigned as a member of cluster and found near the main sequence as shown in Figure 15. Author did not find any sign of regular pulsation for it. A speck of stellar brightness for this variable star has detected on date 11 December 2013 as depicted in Figure 9. The period of this variable star can not be computed by the codes of 'PERIOD04' and 'PerSea'. Thus, this variable star is suggested to be an

irregular type variable.

In the case of variable star V_{17} , the comparison stars are ID 2439 ($5^h : 36^m : 14.60^s$, $34^\circ : 07' : 21.1''$) and ID 2479 ($5^h : 35^m : 56.35^s$, $34^\circ : 05' : 53.3''$). The comparative light curves of both comparison stars has almost constant difference of brightness during observation of each night. Comparative light curves of V_{17} with its comparison stars indicate that spacing of light curves are varying night to night as depicted in the middle Set of Panels of Figure 9. It may be due to character of long variability of V_{17} with irregular pulsation. In addition, the light curves of star ID 2439 also show a character of long term variability.

10.8.2 Star IDs 2868, 2875 (V_{18}) and 2889 of NGC 1960

The variable star V_{18} is a cluster member due to its kinematic probability (0.764) of membership and distance (1.191 ± 0.065 kpc). Light curves of variable star V_{18} do not show any sign of periodic pulsation. As per observation on date on date 11 December 2013, flare type structure is detected in the constructed light curve of this variable star. Its location found near the main sequence in ($U - B$) vs ($B - V$) TCD and depicted in Figure 15. The codes of 'PERIOD04' and 'PerSea' do not enable to compute period for this variable star. As a result, it is classified as irregular variable star with eruptive phenomena.

In the case of V_{18} , the comparison stars are ID 2868 ($5^h : 36^m : 34.54^s$, $34^\circ : 08' : 31.6''$) and ID 2889 ($5^h : 35^m : 55.53^s$, $34^\circ : 07' : 52.2''$). Due to the almost constant brightness in the light curves for star ID 2868, it is assigned as the standard star. The black comparative light curve of filed stars does not show any noticeable fluctuation in flux, whereas, comparative light curves of V_{18} variable and filed stars confirm the long term stellar variability of V_{18} as depicted in the lower set of panels of Figure 9.

11 Results and Discussion

The contamination of fluxes of fainter stars is occurred due to their nearby brighter stars. Author also found very high scatter data points in the light curves of brighter stars of NGC 1960 due to their unresolved centers in the present deep photometric observations. As a result, author did not analysis the time series observations of brighter and their nearby stars.

Star IDs 1124, 1197, 1348 and 2868 of M36 have approximately constant stellar magnitude during whole observations, their celestial coordinates are ($5^h : 36^m :$

28.92^s, 34^o : 13' : 23.2''), (5^h : 36^m : 25.21^s, 34^o : 13' : 04.1''), (5^h : 36^m : 29.70^s, 34^o : 04' : 53.6'') and (5^h : 36^m : 34.54^s, 34^o : 08' : 31.6'') respectively. Thus, these stars are classified as the standard stars within cluster. As per GAIA database, the distance of stars 1124, 1197, 1348 and 2868 has been computed as 1.166±0.035 *kpc*, 1.152±0.036 *kpc*, 3.461±0.278 *kpc* and 1.419±0.109 *kpc* respectively. Thus, star IDs 1124 and 1197 are members of cluster NGC 1960.

Among the 18 detected variable stars, only four are cross matched with JO20, whereas three of the 36 selected comparison stars are cross matched with JO20, whom stellar variability has not been confirmed in the present analysis. Thus, we concluded that the time series data of one night may leads an over-estimation of short periodic variables via absolute/standard photometry. Since computed value of period for variable star V₃ of cluster DO14 is found to be nearly equal to time duration of its observation, therefore author did not classify this star as per period.

JO20 has used continuous time series data less than 3.5 hours for each observational night, whereas author has additional time series data of 5.4, 7.6, 7.2 and 5.6 hours as observed on dated 11-12-2013, 20-12-2013, 12-01-2015 and 08-02-2015 respectively. Since period value of variable star V₂ of M36 by JO20 is seems to be inaccurate in the view of additional data, therefore it is avoided to classify those variable stars, that have approximately same/ slightly longer period than the time duration of observation for a particular night.

In the case of DO14, author has constructed light curves for selected comparison stars by magnitude translation of non-standardized field via SSM approach, whereas light curves for selected comparison stars of M36 has constructed by absolute photometry via SSM approach. Their comparative analysis indicate that absolute photometry is a meaningful to search for variable stars in the target filed. SSM approach has given same trends of pseudo-variability for comparison stars in the field of both cluster. As a result, this approach confirms that resulting light curves of comparison stars do not depend on the nature of reference catalogue produced by either standard or instrumental magnitudes of stars.

Long periodic variable have approximately constant stellar magnitude during observations of 5-6 hours and are showing substantial magnitude difference after several days. In this connection, they become potential candidate for comparing their light curves that of short periodic variables.

12 Conclusion

The transformation of apparent magnitude of stars into absolute magnitudes is performed through Secondary

Standardization Methodology (SSM). During absolute photometry, there are no need of comparison stars for any variable star leads a major advantage over the differential photometry. In absolute photometry, errors of computed stellar magnitudes may arise due to aliases of different sky conditions with the estimation errors in transformation coefficients. In this connection, light curves of stars show some variation in brightness. To overcome such difficulties, those stars were rejected as variable stars, for which the brightness is below 3 - σ limit of mean errors. The author has applied the differential photometry over absolute photometry for constructing comparative light curves for similar comparison stars with variable stars. This process is defined as differential-absolute photometry and leads an effective reduction of the effects in comparative light curves due to sky conditions of observational night. Scattering of data points in light curves of each individual variable star has been reduced by applying the average moving procedure. This procedure is effective to increase the smoothness of light curves and author proposed a parameter 'structure constant' to measure the smoothness. In the present analysis, the values of structural constant for variables are found to be directly proportional to the smoothness of phase diagrams.

The present analysis is dedicated to find the short periodic variable stars, having period less than 1 day. In this connection, author did not present any analysis for the classification of potential candidate of variable stars with the character of long periodic and irregular variability. To find small periodic variables, time series data for DOLIDZE 14 and NGC 1960 have been collected over one and five nights of observations, respectively. In this connection, the stellar light curves for NGC 1960 and DOLIDZE 14 are extracted from these time series data.

By deep investigate of stellar light curves, a total of 18 and 4 variable stars have been identified in the field of view of cluster NGC 1960 and DOLIDZE 14 respectively. Variables of DoLIDZE 14 consist of one miscellaneous, one rotational, two *binary* type variable stars. There are four *Ellipsoidal*, three *RRc*, two rotational, two *irregular*, two $\delta - Scuti - \gamma - Dor$, two *LADS*, a planet transit, a γDor , a *EB* type variable stars out of 18 short periodic variable stars of NGC 1960 as discussed in section 10. Four of these 18 variable stars are cross matched with JO20. In addition, other three variable stars of JO20 are not found short pulsation stars in present analysis. To carry out the membership analysis for variable stars, the mean proper motion of NGC 1960 and DOLIDZE 14 in their RA and DEC directions were estimated as (0.314±0.026 *mass/yr* and -2.333±0.037 *mass/yr*) and (1.050±0.083 *mass/yr*

and $-2.254 \pm 0.093 \text{ mass/yr}$), respectively.
Due to the observational limitations of CCD camera of 1.04 m telescope at ARIES, a telescope equipped with a very high-capacity CCD camera is needed to carry out the task of searching for sign of variability in the brighter stars of NGC 1960.

13 Competing interest

The authors declare that they have no competing interest.

14 Consent for publication

Not applicable.

15 Ethics approval and Consent to participate

Not applicable.

Acknowledge

GCJ acknowledges the web-portal services of SIMBAD, VIZIER and ESO. Collection and observation of time series data of both clusters (NGC 1960 and DOLIDZE 14) performed by GCJ during 18 September 2012 to 27 April 2015. Director, ARIES gave permission to GCJ to use ARIES Data for research work via letter no. AO/2018/41 on date 12 April 2018.

References

- Alter, G., Balazs, B., Ruprecht, J., Akademiai Kiada, Budapest, P. 3086, 2nd edition (1970). VizieR online Data Catalog, VII/5A.
- Balona, L. A., Guzik, J. A., Uytterhoeven, K., Smith, J. C., Tenenbaum, P., Twicken, J. D., The Kepler view of γ Doradus stars, *MNRAS*, **415**, 3531 (2011)
- Balona, L. A., Baran, A. S., Daszynska-Daszakiewicz, J., De Cat, P., Analysis of *Kepler* B stars: rotational modulation and Maia variables, *MNRAS*, **451**, 1445 (2015)
- Barkhatova K. A., Zokharova P. E., Shaskina L. P. & Orsknova L. K., Some Kinematic parameters of open cluster systems, *Astron. Zh.*, **62**, 854 (1985)
- Buchhave, L. A., Latham, D. W., Johansen, A. et al., An abundance of small exoplanets around stars with a wide range of metallicities, *Nature*, **486**, 375 (2012)
- Catelan, M., Pritzl, B. J., Smith, H. A., The RR Lyre Period-Luminosity Relation. I. Theoretical Calibration, *The Astrophysical Journal Supplement Series*, **154(2)**, 633 (2004)
- Cantat-Gaudin T., & Anders, F., Clusters and Mirages: cataloguing stellar aggregates in the Milky Way, *Astronomy and Astrophysics*, **633**, A99 (2020)
- Carpano, S., Aigrain, S., Favata F., Detecting planetary transits in the presence of stellar variability-optimal filtering and the use of colour information, *A & A*, **401(2)**, 743 (2003)
- Chian B. & Zhu G., An Investigation on the Proper-Motions of the Open Clusters NGC 1960, NGC 6530 and NGC 7380, *Annals of the Sheshan Section of the Shanghai Observatory*, **26**, 53 (1966)
- Clement, C. M., Muzzin, A., Dufton, Q., Ponnampalam, T., Wang, J., Burford, J., Richardson, A., Rosebery, T., Rowe, J. and Hogg, H. S., Variable stars in Galactic Globular Clusters, *The Astronomical Journal*, **122**, 2587 (2001)
- Conrad, C., Scholz R.-D., Kharchenko, N. V. et al. A RAVE investigation on Galactic open clusters. II. Open cluster pairs, groups and complexes, *Astronomy and Astrophysics*, **600**, A106 (2017)
- Delgado, A. J., Alfaro, E. J., Garrido, R., Garcia-Pelayo, J. M., Search for B-Type variables stars in open clusters, *Information Bullatine on Variable Stars(IBVS)*, **2603**, 1 (1984)
- Dias W. S., Monteiro H., Caetano, T. C., Lepine, J.R.D., Assafin, M. Oliveira A. F., Proper motions of the optically visible open clusters based on the UCAC4 catalog, *Astronomy and Astrophysics*, **564**, A79 (2014)
- Dupret, M. A., Grigahcene, A., Garrido, R., Gabriel, M., Scufflaire, R., Theoretical instability strips for δ Scuti and γ Doradus syars, *A&A*, **414(2)**, L17 (2004)
- Freedman, W. L., Madore, B. F., The Hubble constant, *Annual Review of Astronomy and Astrophysics*, **48**, 673 (2010)
- Gaia collaboration et al., *A&A*, **595**, A2 (2016)
- Gaia collaboration et al., *A&A*, **649**, A1 (2021)
- Hanson, M.M., ZAMS O Stars, (Boulder-Munich II: Properties of Hot, Luminous Stars, Edited by Ian) ASP Conference Series 1998, 131-1.
- Hartman, J.D., Gaudi, B.S., Holman, M.J., McLeod, B.A., Stanek, K.Z., Barranco, J.A., Pinsonneault, M.H., Kalirai, J.S., Deep MMT Transit Survey of the Open Cluster M37. II. Variable Stars., *The Astrophysical Journal*, **675**, 1254 (2008)
- Hasan P., Kilambi G. C. & Hasan S. N., Near Infrared Photometry of the Young star clusters NGC 1960, NGC 2453 and NGC 2384, *Bull. Astr. Soc. India*, **33**, 151 (2005)
- Hippke M., Learned J. G., Zee A., Edmondson W. H., Lindner J. F., Kia B., Ditto W. L., and Stevens I. R., Pulsation period variations in the RRc Lyrae star KIC 5520878, *ApJ*, **798**, 42 (2015)
- Jeffries, R. D., Naylor, T., Mayne, N. J., Bell, C. P. M. and Littlefair, S. P., A lithium depletion boundary age of 22 Myr for NGC 1960, *MNRAS*, **434(3)**, 2438 (2013)
- Johnson, H. L., The Galactic Cluster, NGC 2244., *AJ*, **136**, 1135 (1962)
- Johnson H. L. & Morgan W. W., Fundamental stellar photometry for standards of spectral type on the Revised System of the Yerkes Spectral Atlas, *Astrophysical Journal*, **117**, 313 (1953)
- Joshi, Gireesh C., Dynamic Properties and Search of Variable Stars: NGC 1960, In: Mishra, G.C. editor. National Conference on Innovative Research in Chemical, Physical, Mathematical Sciences, Applied Statistics and Environment Dynamics (CPMSED-2015), Krishni Sanskriti Publications (New Delhi) ISBN: 978-93-85822-07-0; 2015, p. 22-27.
- Joshi, Gireesh C., Implication of Phase-folded Diagrams for Validation of the Nature of Stellar Variability I: the case of NGC 6866, *Bulgarian Astronomical Journal*, **37**, 01 (2022)
- Joshi, Gireesh C. & Tyagi, R. K., Statistical analysis for precise estimation of Structural Properties of NGC 1960, *Mathematical Sciences Int Research Journal*, **4**, 384 (2015)
- Joshi, Gireesh C. & Tyagi, R. K., Dynamical Features of Open Star Clusters: DOLIDZ 14, In: Mishra, G.C. editor. International Conference on Recent Trends in Applied Physical, Chemical Sciences, Mathematical/Statistical and Environmental Dynamics (PCME-2015) (ISBN: 978-81-930585-8-9), 2015, p. 37-42.
- Joshi, Gireesh C., Joshi, Y. C., Joshi, S., Tyagi, R. K., Basic Parameters of open star clusters DILIDZE 14 and NGC 110 in infrared bands, *New Astronomy*, **40**, 68 (2015)
- Joshi, Y. C., Joshi, S., Kumar, B., Mondal, S., Balona, L. A., *MNRAS*, **419**, 2379 (2012).
- Joshi, Y. C., Maurya, J., John, A. A., Panchal, A., Joshi, S. and Kumar, B., Photometric, Kinematic and Variability study in the young open cluster NGC 1960, *MNRAS*, **492**, 3602 (2020)
- Kharchenko N. V., Piskunov A. E., Roeser S., Schilbach E. & Schola R.-D., Astrophysical supplements to the ASCC-2.5 II. Membership probabilities in 520 Galactic open cluster sky areas, *Astron. Nachr.*, **325**, 740 (2004)
- Kovacs, G., Zucker, S., Mazeh, T., A box-fitting algorithm in the search for periodic transits, *A&A*, **391**, 369 (2002)
- Landolt A. U., *AJ*, **104**, 340 (1992)
- Lata S., Yadav R. K., Pandey A. K., Richichi A., Eswaraiyah C., Kumar B., Kappellmann N. and Sharma S., Main-sequence variable stars in Young open cluster NGC 1893, *MNRAS*, **442(1)**, 273 (2014)

- Lomb, N., Least-squares frequency analysis of unequally spaced data, *AP&SS*, **39(2)**, 447 (1976)
- Luo, Y. P., Variable stars in the open cluster NGC 2141, *RAA*, **15(5)**, 733 (2015)
- Luo Y. P., Zhang X. B., Deng L. C., and Han Z. W., Discovery of 14 new slowly pulsating b stars in the open cluster NGC 7654, *ApJ Letters*, **746**, L7 (2012)
- Majaess, D. J., Turner, D. G., Lane, D. J., Characteristics of the Galaxy according to Cepheids, *MNRAS*, **398(1)**, 263 (2009)
- Meurers J., Ein Stern-Aggregat im M 36. Mit 7 Textabbildungen, *Z Astrophysics*, **44**, 203 (1958)
- Nilakshi, Sagar R., Pandey A. K. & Mohan V., A study of spatial structure of galactic open star clusters, *A&A*, **383**, 153 (2002)
- Plavchan, P., Jura, M., Kirkpatrick, J. D., Cutri, R. M., Gallagher, S. C., Near-Infrared Variability in the 2MASS Calibration Fields: A search for planetary transit candidates, *The Astronomical Journal Supplement Series*, **175**, 191 (2008)
- Ransom, S. M., Eikenberry, S. S., & Middleditch, J., Fourier Techniques for Very Long Astrophysical time-series analysis, *AJ*, **124**, 1788 (2002)
- Samus, N. N., Kazarovets, E. V., Durlevich, O. V., Kireeva, N. N., Pastukhova, E. N., General catalogue of variable stars: Version GCVS 5.1, *Astronomy Reports*, **61**, 80 (2017)
- Sanner, J., Altmann, M., Brunzendorf, J., Geffert, M., Photometric and kinematic studies of open star clusters. II. NGC 1960 (M 36) and NGC 2194, *A&A*, **357**, 471 (2000)
- Sariya, D. P., Lata, S., Yadav, R. K. S., Variable stars in the globular cluster NGC 4590 (M 68), *New Astronomy*, **27**, 56 (2014)
- Scargle, J. D., Studies in astronomical time series analysis. II. Statistical aspects of spectral analysis of unevenly spaced data, *ApJ*, **263**, 835 (1982)
- Skrutskie, M. F., Cutri, R. M., Stiening, R., et al., The Two Micron All Sky Survey (2MASS), *AJ*, **131**, 1163 (2006)
- Sharma S., Pandey A. K., Ogura K., Mito H., Tarusawa K. & Sager R., Wide-field CCD photometry around nine open clusters, *AJ*, **132**, 1669 (2006)
- Sharma S., Pandey A. K., Ogura K., Aoki T., Pandey K., Sandhu T. S. & Sager R., Mass functions and photometric binaries in nine open clusters, *AJ*, **135**, 1934 (2008)
- Smith, R., Jeffries, R. D., Dust discs around intermediate-mass and Sun-like stars in the 16 Myr old NGC 1960 open cluster, *MNRAS*, **420(4)**, 2884 (2012)
- Soszynski, I., Poleski, R., Udalski, A. et al., The Optical Gravitational Lensing experiment. The OGLE-III catalog of variable stars. I. Classical Cepheids in the Large Magellanic Cloud, *Acta Astronomica*, **58**, 163 (2008)
- Stetson P. B., DAOPHOT: A Computer Program for Crowded-Field Stellar Photometry, *PASP*, **99**, 191 (1987)
- Stetson P. B., 1992 in ASP conf. Ser. vol. 25, *Astronomical Data Analysis Software and System*, I. Astron. Soc. Pac., ed. Warrall D. M., and Biemesderfer C., Barnes J., San Francisco, 297
- Wood, P. R. and Sebo, K. M., On the pulsation mode of Mira variables: evidence from the Large Magellanic cloud, *MNRAS*, **282(3)**, 958 (1996)
- Wright E. L., Eisenhardt P. R. M., Mainzer A. K., et al., The Wide-field Infrared Survey Explorer (WISE): Mission Description and Initial On-orbit Performance, *AJ*, **140**, 1868 (2010)